Clinical and Translational Report

The Rational Development of CD133-Targeting Immunotherapies for Glioblastoma

Graphical Abstract
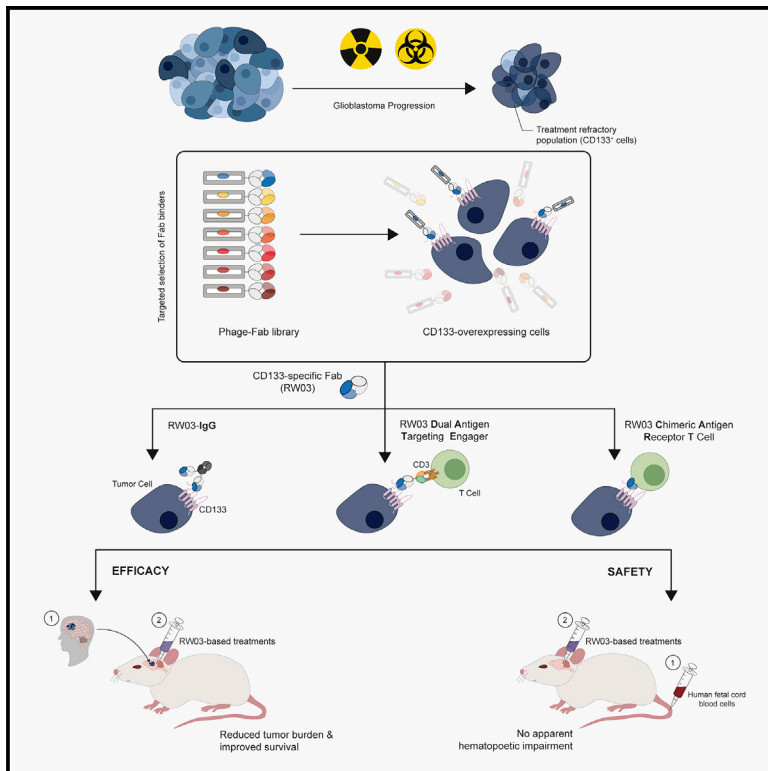
Authors

Parvez Vora, Chitra Venugopal, Sabra Khalid Salim, ..., Kristin Hope, Jason Moffat, Sheila Singh

Correspondence

ssingh@mcmaster.ca (S.S.), j.moffat@utoronto.ca (J.M.)

In Brief

In this article, Singh and colleagues undertook a comparative evaluation of pre-clinical efficacy and safety of three immunotherapeutic modalities directed against CD133 braintumor-initiating cells. While all three modalities were efficacious in orthotopic GBM xenografts, CD133-specific CAR-T cells represented the most therapeutically tractable strategy against functionally important CD133+ GBM cells.

Highlights

- Three immunotherapeutic modalities were developed to target CD133+ cells

- Anti-CD133 DATEs and CAR-T cells are active in patient-derived glioblastoma (GBM) models

- CD133-specific CAR-T (CART133) has enhanced activity in orthotopic GBM xenograft models

- Intra-tumoral CART133 does not induce acute systemic toxicity in humanized mouse models

CellPress

Clinical and Translational Report

The Rational Development of CD133-Targeting Immunotherapies for Glioblastoma

Parvez Vora,[1,6] Chitra Venugopal,[1,6] Sabra Khalid Salim,[1,5] Nazanin Tatari,[1,5] David Bakhshinyan,[1,5] Mohini Singh,[1,5] Mathieu Seyfrid,[1,6] Deepak Upreti,[1,6] Stefan Rentas,[1,5] Nicholas Wong,[1] Rashida Williams,[2] Maleeha Ahmad Qazi,[1,5] Chirayu Chokshi,[1,5] Avrilynn Ding,[1] Minomi Subapanditha,[1] Neil Savage,[1,5] Sujeivan Mahendram,[1,6] Emily Ford,[1] Ashley Ann Adile,[1,5] Dillon McKenna,[1,6] Nicole McFarlane,[1] Vince Huynh,[4] Ryan Gavin Wylie,[4] James Pan,[2] Jonathan Bramson,[3] Kristin Hope,[1] Jason Moffat,[2,7,*] and Sheila Singh[1,5,6,7,8,*]

[1]McMaster Stem Cell and Cancer Research Institute, McMaster University, Hamilton, ON, L8S 4K1, Canada
[2]Donnelly Centre, Department of Molecular Genetics, Institute of Biomolecular Engineering, University of Toronto, 160 College Street, Toronto, ON M5S 3E1, Canada
[3]Department of Pathology and Molecular Medicine, McMaster University, 1280 Main St W, Hamilton, ON L8S 4L8, Canada
[4]Department of Chemistry and Chemical Biology, McMaster University, Hamilton ON L8S 4M1, Canada
[5]Departments of Biochemistry and Biomedical Sciences, McMaster University, 1200 Main Street West, Hamilton, ON L8N 3Z5, Canada
[6]Surgery, Faculty of Health Sciences, McMaster University, 1200 Main Street West, Hamilton, ON L8N 3Z5, Canada
[7]Senior author
[8]Lead Contact
*Correspondence: ssingh@mcmaster.ca (S.S.), j.moffat@utoronto.ca (J.M.)
https://doi.org/10.1016/j.stem.2020.04.008

SUMMARY

CD133 marks self-renewing cancer stem cells (CSCs) in a variety of solid tumors, and CD133+ tumor-initiating cells are known markers of chemo- and radio-resistance in multiple aggressive cancers, including glioblastoma (GBM), that may drive intra-tumoral heterogeneity. Here, we report three immunotherapeutic modalities based on a human anti-CD133 antibody fragment that targets a unique epitope present in glycosylated and non-glycosylated CD133 and studied their effects on targeting CD133+ cells in patient-derived models of GBM. We generated an immunoglobulin G (IgG) (RW03-IgG), a dual-antigen T cell engager (DATE), and a CD133-specific chimeric antigen receptor T cell (CAR-T): CART133. All three showed activity against patient-derived CD133+ GBM cells, and CART133 cells demonstrated superior efficacy in patient-derived GBM xenograft models without causing adverse effects on normal CD133+ hematopoietic stem cells in humanized CD34+ mice. Thus, CART133 cells may be a therapeutically tractable strategy to target CD133+ CSCs in human GBM or other treatment-resistant primary cancers.

INTRODUCTION

Glioblastoma (GBM) is the most common primary adult malignant brain tumor that remains incurable despite maximal safe surgical excision and chemo-radiotherapy. Therapeutic failure in GBM is, in part, due to intratumoral heterogeneity (ITH) (Bao et al., 2006; Chen et al., 2012), which has been systematically interrogated by The Cancer Genome Atlas (TCGA) project. The TCGA classification has offered insights into the genetic regulation of GBM, and patterns of gene expression have been collated to identify molecular subgroups with putative prognostic or predictive significance. However, its impact on treatment and prognosis has been limited by the continuous spatial and temporal evolution of the tumor's genetic landscape, generating an unimaginable degree of cellular heterogeneity within a single tumor (Burrell et al., 2013; Meyer et al., 2015; Suvà et al., 2014; Swanton, 2015). The clonal evolution of cancer may be regulated by determinants of stemness—specifically, self-renewal—and cur-

rent therapies have not considered how genetic perturbations or surface markers affect such functional processes. Furthermore, poor patient survival correlates with marker expression of cancer stem cells (CSCs) or tumor-initiating cells (TICs), which are also implicated in the development of treatment resistance in many malignancies (Corbin et al., 2011; Diehn et al., 2009; Dylla et al., 2008; Meacham and Morrison, 2013; Oravecz-Wilson et al., 2009), including GBM. Within the evolution of GBM, the pentaspan transmembrane glycoprotein CD133 may mark cells with various properties necessary for tumor initiation, persistence, and recurrence.

A marker of hematopoietic (Skorzewska et al., 1989) and neural (Uchida et al., 2000) stem cells, CD133 also identifies TIC populations in multiple human cancers (Cox et al., 2009; Hermann et al., 2007; Lai and Singh, 2004; O'Brien et al., 2007). CD133 expression correlates with disease progression, metastasis, recurrence, and poor overall survival in several human malignancies (Shibahara et al., 2013; Zeppernick et al., 2008; Zhang

et al., 2012); however, insight into its function remains limited (Mak et al., 2012; Wei et al., 2013). Although CD133 is the first identified member of the Prominin family of pentaspan membrane glycoproteins with an implied signaling role, the functional significance of CD133 in modulating ITH via self-renewal regulation remains elusive. However, CD133 has proven to be a necessary and sufficient factor in enabling GBM cells to adapt to current therapies, transit between different clonal populations of tumor cells, and outcompete neighboring cells based on phenotypic differences in stemness (Venugopal et al., 2015).

After CD133 was identified as a marker of brain tumor-initiating cells (BTICs) (Singh et al., 2003, 2004), CD133+ GBM BTICs were subsequently found to be resistant to radiotherapy (Bao et al., 2006) and chemotherapy (Liu et al., 2006). BTICs that escape treatment may explain why almost all patients relapse despite aggressive current therapies. A low-frequency CD133+ subclone may initiate the tumor and then persist throughout treatment by generating a cellular hierarchy that contributes to ITH and the acquisition of drug resistance. Whereas current radiotherapy and chemotherapeutic agents may debulk the bottom of the cellular hierarchy, cells endowed with a CD133-driven self-renewal phenotype could escape such therapies and re-emerge to initiate tumor relapse. A similar paradigm in acute myeloid leukemia describes rare hematopoietic stem cells that acquire pre-leukemic mutations that are able to regenerate the heterogeneous leukemic landscape and maintain a clonal reservoir of treatment-resistant cells implicated in leukemic progression and relapse (Shlush et al., 2014). The presence of these ancestral leukemic cells at disease onset and recurrence highlights self-renewal as an essential process by which these cells persist throughout tumorigenesis. Given that self-renewal is largely measured by functional assays that require proliferation, the identification of targeted therapies that affect both self-renewal and proliferation has been increasingly difficult (Kreso et al., 2014; Sachlos et al., 2012). This has been especially true in GBM, where self-renewal regulators identified in transgenic mouse models have been of limited clinical utility (Zhu et al., 2014).

We have previously shown that a higher self-renewal index correlates with reduced GBM patient survival (Venugopal et al., 2012). Recent reports suggest that CD133 is a prognostic biomarker for relapse (Shibahara et al., 2013), time to malignant progression from low-grade gliomas, and poor survival (Zeppernick et al., 2008). Analyses of our brain tumor tissue bank composed of patient-derived GBM tumor samples show variable expression of CD133 (Figure S1A; Table S1). The TCGA glioma database shows higher expression of CD133 in GBM (grade IV glioma) compared to low-grade glioma and in the proneural and classical subgroups compared to the mesenchymal subgroup (Figure S1B). More importantly, CD133^{high} GBM patients grouped under the proneural and classical subgroups have significantly poorer survival compared to CD133^{low} GBM patients (Figure S1C). Hence, the clinical utility of CD133 as a prognostic GBM biomarker needs to be explored further. When expressed in a minority cellular subpopulation of a tumor, CD133 marks a TIC population capable of driving aggressive tumor growth, possibly using asymmetric self-renewal. Disabling the CD133 subpopulation (regardless of high or low expression level in any given tumor) shows abrogation of tumor growth and survival benefit in preclinical models (Cox et al., 2009; Hermann

et al., 2007; O'Brien et al., 2007). In principle, therapeutic targeting of such a functionally relevant driver of aggressive tumor growth and ITH may not require uniform or extremely high level of expression in tumor cells to yield clinical benefit.

Several groups have demonstrated that targeting of CD133+ BTICs is a clinically tractable therapeutic strategy in brain cancer. By undertaking *in silico* screens with small-molecule inhibitors and connectivity mapping of a CD133 signature from pooled GBM transcriptomes, we undertook proof-of-concept experiments to show that pyrvinium selectively targeted self-renewing, chemo-radioresistant, and functionally important CD133+ GBM cells that drive post-treatment recurrence (Venugopal et al., 2015). However, immunotherapeutic approaches present potentially more specific and effective means to target the cell-surface proteins and may have particular advantages in targeting CSCs. Immunotherapy is not dependent on any known mechanisms that CSCs use to evade conventional therapy, including assuming a quiescent state to escape anti-proliferative chemotherapy and radiotherapy, upregulation of cell-surface transporters to efflux chemotherapies, or major histocompatibility complex class I (MHC-I) downregulation to evade immunosurveillance. Immuno-therapeutic methods targeting CD133+ BTICs range from conjugating the anti-CD133 monoclonal antibody AC133 to immuno-toxins (Waldron et al., 2011, 2014), CD133-targeting natural killer cells (Schmohl et al., 2016a, 2016b), dendritic cell therapies (Rudnick et al., 2017), bispecific T cell engagers (Prasad et al., 2015), and chimeric antigen receptor T cell (CAR-T cell) therapy (Wang et al., 2018; Zhu et al., 2015). Niedermann and colleagues (Zhu et al., 2015) designed an AC133-specific CAR-T cell that recognizes and kills GBM cell lines overexpressing CD133 and patient-derived GBM stem cells and that shows efficacy in an orthotopic GBM stem cell nude mouse model. However, evaluation of treatment efficacy in these models may have been hindered by rejection of human T cells by residual murine immune cells in nude mice. In this work, we compare three immunotherapeutic modalities (CAR-T cell, dual-antigen T cell engager [DATE] antibody, and monoclonal antibody) in the therapeutic targeting of GBM against the novel anti-CD133 epitope, detectable by the engineered human antibody RW03. These therapies were delivered via intra-tumoral/local-regional route to highly immunosuppressed NSG mice engrafted with minimally cultured patient-derived tumor cells, representing a clinically relevant model to address tumor heterogeneity, tumor cell clonal evolution, and the importance of cell-cell and cell-extracellular matrix interactions within the tumor microenvironment, and they predicted patient response to treatment.

RESULTS AND DISCUSSION

Generation of Anti-CD133 Human Synthetic Antibody RW03

Immunodetection of CD133 has presented a major limitation toward therapeutic development, as currently available antibodies are limited in their ability to detect CD133 splice variants and aberrantly post-translationally modified CD133. We used iterative cell-based panning, which combines the use of matched HEK293 and HEK293-CD133-overexpressing cells (Mak et al., 2011), a phage-displayed synthetic antibody fragment (Fab) library (Nixon et al., 2019; Persson et al., 2013), and DNA sequencing, to identify

A
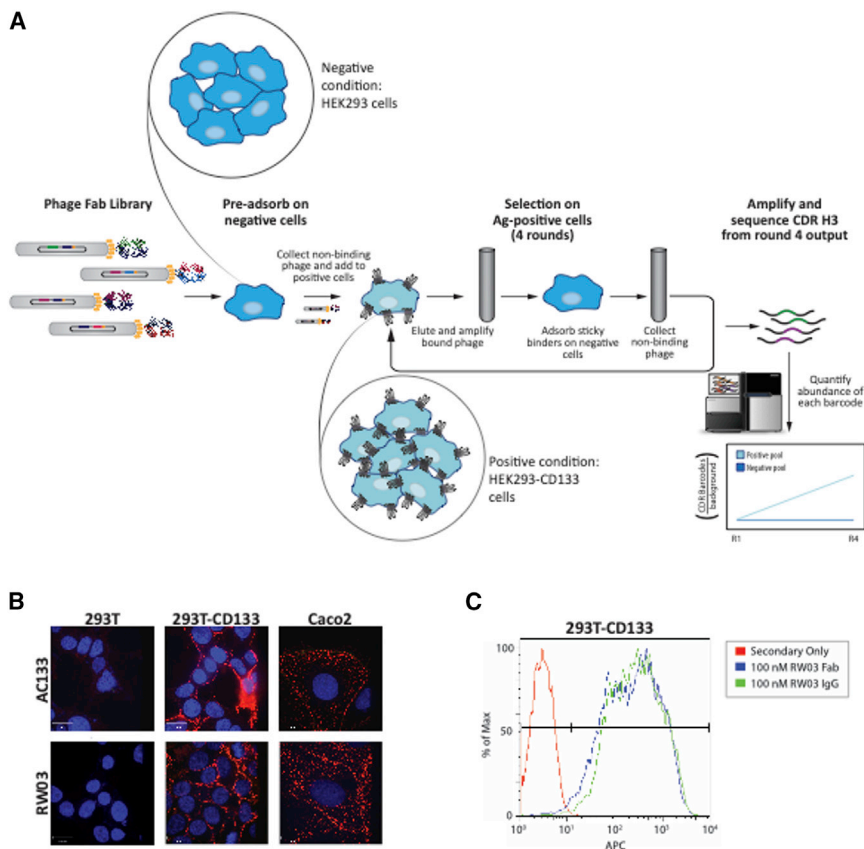
Figure 1. Generation of Anti-CD133 Human Synthetic Antibody RW03

(A) Workflow of CellectSeq strategy used to raise CD133-specific Fab-phage from Library F. A nested PCR amplifies a region encompassing the heavy and light variable regions. Parallel PCR reactions are set up using primers specific to the CDRL3 and CDRH3 regions. The CDR-specific products are amplified, digested, and ligated into an expression vector.

(B) Immunofluorescence assays show AC133 and RW03 Phage-Fab clones binding to the HEK293-CD133 overexpressing line and colorectal adenocarcinoma line Caco-2 specifically with no detectable background binding to the HEK293 cell line.

(C) Both RW03 Fab (blue line) and RW03 IgG (green line) can identify endogenously expressed CD133 cells by flow cytometry. Red line indicates secondary-only binding.

B

C

Fabs targeting human CD133, encoded by the *PROM1* gene (Figure 1A). This effort yielded a Fab called RW03 (i.e., RW03-Fab), which demonstrated highly specific binding to the CD133-overexpressing cells with minimal binding to the parental HEK293-CD133-non-expressing cells. The RW03-Fab was converted to a full-length human immunoglobulin G (IgG)1 (RW03-IgG, hereinafter), and immunofluorescence and flow cytometry were performed on HEK293-CD133, Caco-2 cells, as well as on several other cancer cell lines, to determine binding specificity and affinity. RW03-IgG showed prominent binding to the plasma membrane, internal vesicles, and membrane protrusions by immunofluorescence (Figure 1B). RW03-IgG was also validated using flow cytometry, and the effective half-maximal binding concentration was calculated to be 0.5 nM (Figure 1C). RW03-IgG was also confirmed to bind several different cultured cell models, including patient-derived GBM cells (data not shown).

In Vitro and *In Vivo* Efficacy of Anti-CD133 Human Synthetic Antibody

To assess the therapeutic potential of RW03-IgG in GBM, we performed secondary sphere formation assays to measure clonogenicity, as well as proliferation assays. Upon *in vitro* treatment of patient-derived GBM cells with RW03-IgG, we saw a marked reduction in clonogenicity in a dose-dependent manner (Figure 2A). However, RW03-IgG treatment failed to block proliferation of GBM cells across multiple concentrations (Figure 2B). We then sorted GBMs into CD133+ and CD133− fractions and found that RW03-IgG treatment did reduce the secondary

sphere formation ability of the CD133− GBM subpopulation (Figure 2C). However, the RW03-IgG treatment failed to block the proliferation potential of either population (Figure 2D).

The blood-brain barrier (BBB) poses a unique challenge for effective drug delivery to the brain. Local delivery strategies, including bolus injections or use of convection-enhanced delivery, have been extensively evaluated for delivery of therapeutic biologics, liposomes, and viral-mediated and cellular therapies (Bobo et al., 1994; Bogdahn et al., 2011; Brown et al., 2015; Ding et al., 2010a, 2010b; Priceman et al., 2018). Hence, we evaluated the therapeutic potential of various modalities delivered by a local intra-tumoral route of administration in the human xenograft model of GBM. Patient-derived early-passage GBM cells were engrafted intracranially in non-obese diabetic (NOD) severe combined immunodeficiency (SCID)-gamma (NSG) mice, and upon confirmation of half-maximal engraftment, the xenografted mice were intracranially injected with twice-weekly doses of RW03-IgG, at 100 μg per dose. Although nonsignificant, we observed some reduction in the tumor burden of mice treated with RW03-IgG compared to control IgG after four doses of treatment (Figure 2E). While the mode of action *in vivo* still remains to be studied, one possibility is that RW03-IgG transiently impacts the clonogenic potential of the CD133+ GBM cells because of the shorter half-life compared to cellular therapies. Pharmacodynamic studies using a 1-compartment model, supported by the first-order elimination process, show an elimination rate constant (k_e) of 0.0443 ± 0.099 h^{-1} for RW03-IgG (Figure S2). From k_e, the antibody has a half-life ($t_{1/2}$) of 15.6 h, which is similar to reported antibody $t_{1/2}$ values with minimal Fc receptor (12.8 h) binding within brain tissue (O'Hear and Foote, 2006; Wolak et al., 2015), suggesting that RW03-IgG clearance is not Fc-receptor-mediated elimination.

The efficacy of RW03 delivered as a monoclonal antibody revealed insights into the biological function of CD133 in brain
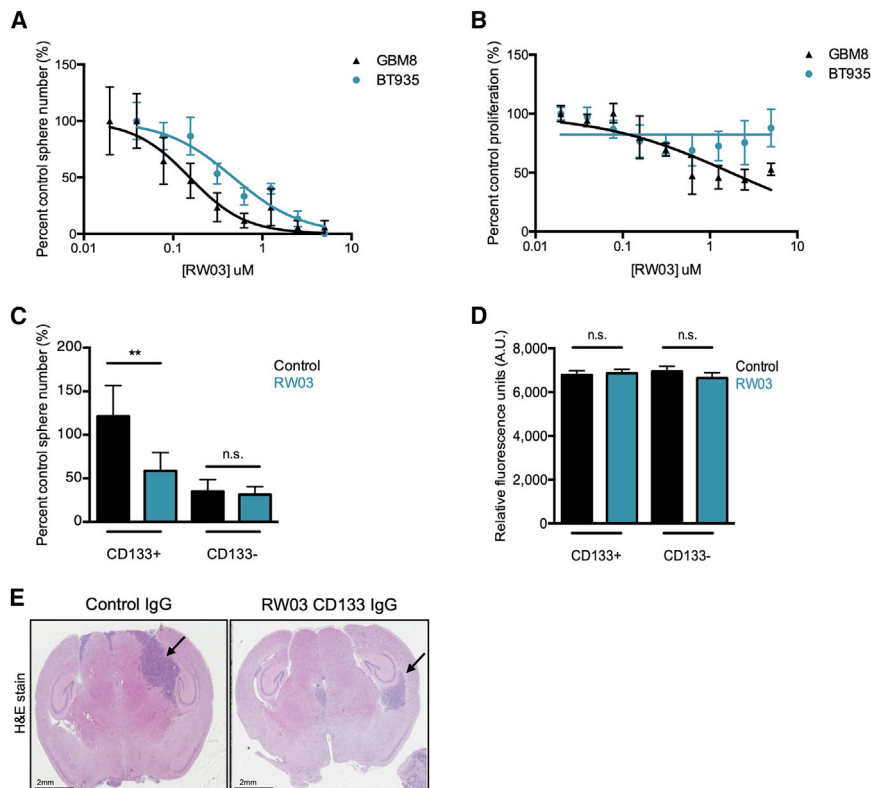
Figure 2. Therapeutic Targeting of CD133+ GBM BTICs Using RW03 IgG

(A) Treatment of CD133^{HIGH} GBMs with varying concentrations of RW03 IgG reveal decreased sphere-forming capacity.

(B) Treatment of CD133^{HIGH} GBMs with varying concentrations of RW03 IgG did not affect proliferative capacity.

(C and D) Treatment of CD133+ and CD133− sorted GBM cells with RW03 did not affect proliferative capacity.

(C) Percent control sphere number (Student's t test; n = 7, p = 0.0011).

(D) Relative fluorescence units are a measure of cell proliferation (Student's t test).

(E) NSG mice that were intracranially implanted with 1 million human CD133+ GBMs showed moderate reduction in tumor burden upon treatment with RW03 IgG compared to control IgG as assessed by H&E staining (n = 34).

dose-dependent manner, validating binding to both antigen-binding surfaces (Figure S3C).

T cell activation evaluation by extracellular staining of peripheral blood mononuclear cells (PBMCs), incubated with patient-derived GBM lines, showed elevated expression of CD25 (a late activation marker) and CD69 (an early activation marker), only in the presence of the CD133 DATE (Figure S3D). T cell activation was associated with the elevation of both cytokines: tumor necrosis factor alpha (TNF-α) and interferon (IFN)γ (Figure S3E). We then assessed the efficacy and potency of the CD133 DATE in a directed T cell cytotoxicity assay targeting GBM culture models where ~95% of the cells express CD133. Co-incubation of PBMCs (suspension) and GBM cells (adherent) at an effector:target (E:T) ratio of 1:1 in the presence of the CD133 DATE led to the killing of GBM cells as evident by microscopic examination (Figure S3F). In contrast to wells without the DATE, the co-cultures with the CD133 DATE saw detachment of target GBM cells that formed rosettes, indicating clumps of dying cells. In addition, a bioluminescence-based cytotoxicity assay was also used to assess the redirected lysis of GBM cells by the CD133 DATE. In this assay, a dose-dependent killing of firefly-luciferase-expressing GBM cells was observed in the cultures with the CD133 DATE, whereas no killing was observed in the control group with no DATE (Figure S3G). The potent activity of the CD133 DATE against CD133+ GBM cells was observed at E:T ratios as low as 1:1 (Figure S3H). Together, these data demonstrate that our CD133 DATE effectively eliminates CD133+ tumor cells in the presence of cytotoxic T lymphocytes.

cancer, as the IgG specifically blocked stem cell self-renewal *in vitro* with no apparent effect on proliferation. CD133 expression in brain cancer cells can be either seen in plasma membrane protrusions and associated with lipid rafts, or seen in endocytic compartments where such cytoplasmic localization predicts poor prognosis in cancer patients (Chen et al., 2017). Therefore, it is assumed that trafficking of CD133 protein between cell surface and intracellular compartment correlates with the dynamic flux of clonal evolution of CSCs through therapy and the physiological property of self-renewal. Thus, an IgG that binds to CD133 at the cell surface may reduce the self-renewal capacity of CSC clonal populations dynamically, resulting in impaired tumorigenicity *in vivo*. We saw a non-significant reduction in GBM tumor burden *in vivo* with RW03 IgG treatment, likely due to abrogation of self-renewal without cytotoxicity, allowing for dynamic recovery of CD133+ BTICs over time.

Activation of T Cells and Redirected Lysis of GBM Cells in Cocultures by CD133 Dual Antigen T Cell Engagers (DATEs)

Results from RW03 IgG treatment led us to hypothesize that a targeted cytotoxic approach was required for the eradication of CD133+ BTICs and subsequent durable reduction of GBM tumor mass. In order to explore the use of the RW03-Fab in another therapeutic binding modality, we generated a DATE. The DATE was engineered by fusing the light chain of the RW03-Fab to OKT3, a single-chain fragment variable (scFv) construct that binds the antigen-binding region of the mitogenic antiCD3ε clone (Figures S3A and S3B) (Shiheido et al., 2014). The purified DATE effectively recognized both CD3 on T cells and CD133 on GBM cells in a

CD133 DATE Inhibits the Growth of Orthotopic Xenografts Initiated from GBM Cells

The antitumorigenic activity of our CD133 DATE *in vivo* was next tested using two early-passage patient-derived GBM models, including BT428 and BT935. Importantly, our CD133 DATE does not cross-react to murine CD133 (also known as Prom1)

Figure 3. Therapeutic Targeting of Patient-Derived GBM Cells Using CD133 CAR-T Cells

(A and B) Schematic representation of CAR structures is presented in (A). Successful transduction of CAR-T vectors is indicated as observed with NGFR+ cells in CAR CON and NGFR+Myc+ cells in CART133 cells. Their representative flow plots are presented in (B).

(C) Activation of T cells was solely observed in CART133 cells in comparison to control CAR-T cells when co-cultured with CD133^{HIGH} GBMs overnight, as confirmed by CD25 and CD69 expression by flow cytometry (n = 3); p = 0.0300 for CD25 and GBM8, p < 0.0001 for CD69 and GBM8, p = 0.00183 for CD25 and BT935], and p < 0.00023 for CD69 and BT935.

(D) CART133 cells show increase in proliferation compared to CAR CON cells after co-culturing with GBM cells (Student's t test; n = 12, p < 0.0001 [CAR-T alone], p < 0.0001 [CAR-T +GBM]).

(E) Cytokine bead array (CBA) show elevated secretion of Th1 and Th2 cytokines in supernatant collected from co-cultures of CART133 and GBM cells.

(F) CART133 cells significantly induce cytotoxicity of CD133^{HIGH} GBMs in comparison to control CAR-T cells after co-culturing for 24 h at low E:T ratios (Two-way ANOVA; n = 3, p < 0.0001).

or murine CD3ε (data not shown). Therefore, we co-injected the DATE with freshlythawed human PBMCs intracranially into immunocompromised NSG mice engrafted with GBM cells confirmed to have brain tumors by magnetic resonance imaging (MRI). In contrast to treatment with PBMCs only, the CD133 DATE treatment resulted in significantly reduced tumor size after four 50-μg doses of CD133 DATE (Figures S4A–S4C). Mice receiving PBMCs only demonstrated rapid tumor growth, with all mice in this group reaching endpoint by 135 days, while the mice that received the CD133 DATE survived more than 160 days (Figure S4D). Although the treatment with the CD133 DATE significantly prolonged the survival of tumor xenografted mice, the animals succumbed to tumor burden after the treatment was terminated. Variable responses in different patient-derived GBM BTIC lines may be the result of different antigen densities on the tumor cell surface. However, all mice showed tu-

mor progression upon completion of treatment, suggesting that the short half-life of DATEs requires development of a yet-to-be optimized dosing regimen. The complex pharmacokinetics and pharmacodynamics of this treatment modality in the setting of a solid invasive tumor requires further investigation for achieving of maximum therapeutic efficacy in GBM. However, these results indicate that use of CD133 DATE in pre-clinical mouse models of GBM could be a viable therapeutic strategy for this disease, consistent with other studies using similar modalities (Choi et al., 2013; Prasad et al., 2015).

Generation and Characterization of CD133-Specific CAR-T Cells

To explore the utility of RW03 in the context of a chimeric antigen receptor T cell (CAR-T cell), we engineered a second-generation CAR-T cell using the RW03 binding sequences (hereinafter

referred to as CART133). We replaced the scFv domain of a previously published HER2-specific CAR-T construct (Hammill et al., 2015; VanSeggelen et al., 2015) with RW03 scFv that binds to human CD133 and utilized the ΔNGFR and c-myc to confirm the efficiency of transduction and surface expression of the CAR targeting CD133, respectively (Figures 3A and 3B).

To determine the functionality of the CART133 cells, we cocultured CART133 or control CAR-T (CAR CON, as described in Figure 3A) cells with CD133+ GBM cells and found that expression levels of CD25 and CD69 were specifically elevated on CART133 cells in the presence of GBM cells expressing CD133. Other combinations of T cells alone or control CAR-T plus GBM cells showed no difference in CD25 and CD69 levels (Figure 3C). We next assessed the ability of CAR-T cells to secrete cytokines and to proliferate in response to antigen stimulation by CD133+ GBM cells. CD3+ CART133 cells cocultured with CD133+ GBM cells were highly proliferative compared to all other control conditions tested (Figure 3D). Furthermore, TNF-α and IFNγ were significantly upregulated in supernatants collected from co-cultures of CART133 and GBM cells (Figure 3E). Together, these data demonstrate robust, antigen-specific CART133 responses upon contact with CD133+ tumor cells.

We next sought to evaluate functional, antigen-specific, cytotoxic responses of CART133 cells against patient-derived GBM cells, in order to demonstrate the specific killing of CD133+ cells. Using the bioluminescence-based cytotoxicity assay described earlier to test CD133 DATEs, we assessed the specific lysis of two different patient-derived GBM models (i.e., GBM8 and BT935) by CART133 cells. Our results demonstrate target antigen specificity, and a dose-dependent response showing significant GBM cell lysis, even at very low E:T ratios, whereas the control CAR-T cells did not show any cytolytic activity toward GBM cells (Figure 3F). Thus, CART133 showed specific and potent activity against CD133+ BTIC lines.

CART133 Exhibited Enhanced Anti-tumor Activity in Orthotopic Xenografts Initiated from GBM Cells
The specificity and effector functions observed for the CART133 in vitro led us to test the in vivo tumor activity of CART133 cells in NSG mice bearing human GBM tumors. Recent clinical trials evaluating the safety of intracranial administration of CAR-T cells for the treatment of GBM have shown promising results, and one case report has shown a dramatic response in a recurrent GBM patient (Brown et al., 2015, 2016, 2018; Priceman et al., 2018). Therefore, we opted to test the efficacy of our CAR-T cells with an invasive local delivery method that bypasses the BBB. Patient-derived, early-passage GBM models, including GBM8, BT428, and BT935 were engrafted intracranially. Upon confirmation of tumor growth by MRI, mice were intracranially injected with two similar doses of either CART133 or control CAR-T cell (1×10^6 effector cells per dose) (Figure 4A). Mice injected with CAR CON cells succumbed quickly to the effects of their brain tumors, whereas mice treated with CART133 cells showed significant tumor reduction (Figures 4B and 4C). The treatment effect was reflected in significantly increased overall survival of xenografted mice treated with CART133 cells (Figure 4D; Figure S5B). CART133 also showed persistence and localization to tumor areas, as detected by CD3 staining in comparison to

CAR CON, which did not show CD3 immunoreactivity in control mice (Figures 4E–4G; Figure S6A). Quantification of NGFR+ CART133 cells revealed that a mean of 200K cells remained in the brain at endpoint. Flow-cytometric analysis of the residual tumor post-treatment also confirmed almost complete elimination of CD133+ GBMs (Figure 4G).

In contrast to DATEs, just two doses of 1×10^6 CAR-T cells engineered against the RW03 epitope exhibited striking efficacy and potent killing, with almost total eradication of the cognate CD133+ cell population in each of our GBM BTIC patient-derived lines. Regardless of the variability of CD133 protein expression across our patient-derived BTICs (BT428, 10.99%; BT935, 95.3%; and GBM8, 91.5%), local delivery of CART133 cells exhibited high efficacy against diffuse infiltrative disease. In contrast to current therapies targeting non-CSC markers such as EGFRvIII and interleukin (IL)-13Rα2 (Brown et al., 2016; O'Rourke et al., 2017), targeting CD133 abrogates a functionally relevant CSC population that may generate ITH through the asymmetric division of a parental CSC into highly variable progeny. As with any CSC targeting strategy, the major limitation is the ability of CD133− tumor cells to initiate tumor formation. Single-cell transcriptome analysis show that GBM CSCs are heterogenous and that a single CSC marker may not be able to distinguish the CSC and non-CSC subpopulations (Patel et al., 2014). However, targeting one of the apex subpopulations in the CSC hierarchy, which is known to be associated with worse prognosis, may significantly slow the GBM tumor progression. Since the discovery of CD133+ BTICs (Singh et al., 2004), other markers including known neural stem cell (NSC) markers, have been shown to identify other BTIC populations including CD15 (Son et al., 2009), ITGA6 (Lathia et al., 2010), CD44 (Anido et al., 2010), and L1CAM (Bao et al., 2008). These markers could be explored further to target a boarder subpopulation of GBM BTICs. Data from clinical studies have continued to support the belief that CD133 is a significant prognostic marker regarding poor overall survival and progression-free survival in brain cancer patients (Han et al., 2016; Li et al., 2017; Venugopal et al., 2015). Combining the standard of care with CD133 CAR-T cell therapy could effectively target CD133− cells, as they have previously been shown to possess increased sensitivity to chemo- and radiotherapy (Bao et al., 2006; Liu et al., 2006). A future combination of CART133 therapy with new and empirically defined targets identifying non-CSC GBM populations will address intra- and inter-tumoral heterogeneity.

CART133 Treatment Does Not Incur Acute Toxicity in Normal Hematopoietic Stem and Progenitor Cells that Express CD133
CD133 is not a tumor-specific antigen and is expressed on various normal stem and progenitor cell populations, including hematopoietic (Yin et al., 1997), neuronal (Uchida et al., 2000), kidney (Sagrinati et al., 2006), and prostate (Leong et al., 2008) stem cells, as well as on a subset of differentiated epithelial cells (Karbanová et al., 2008). Although in healthy adult humans, the percentage of CD133+ stem cells in other systems is very low, any therapy directed against CD133+ cells will need to address the potential impact on hematopoiesis.

Following the demonstration of the therapeutic efficacy of three immunotherapeutic modalities against CD133 in our
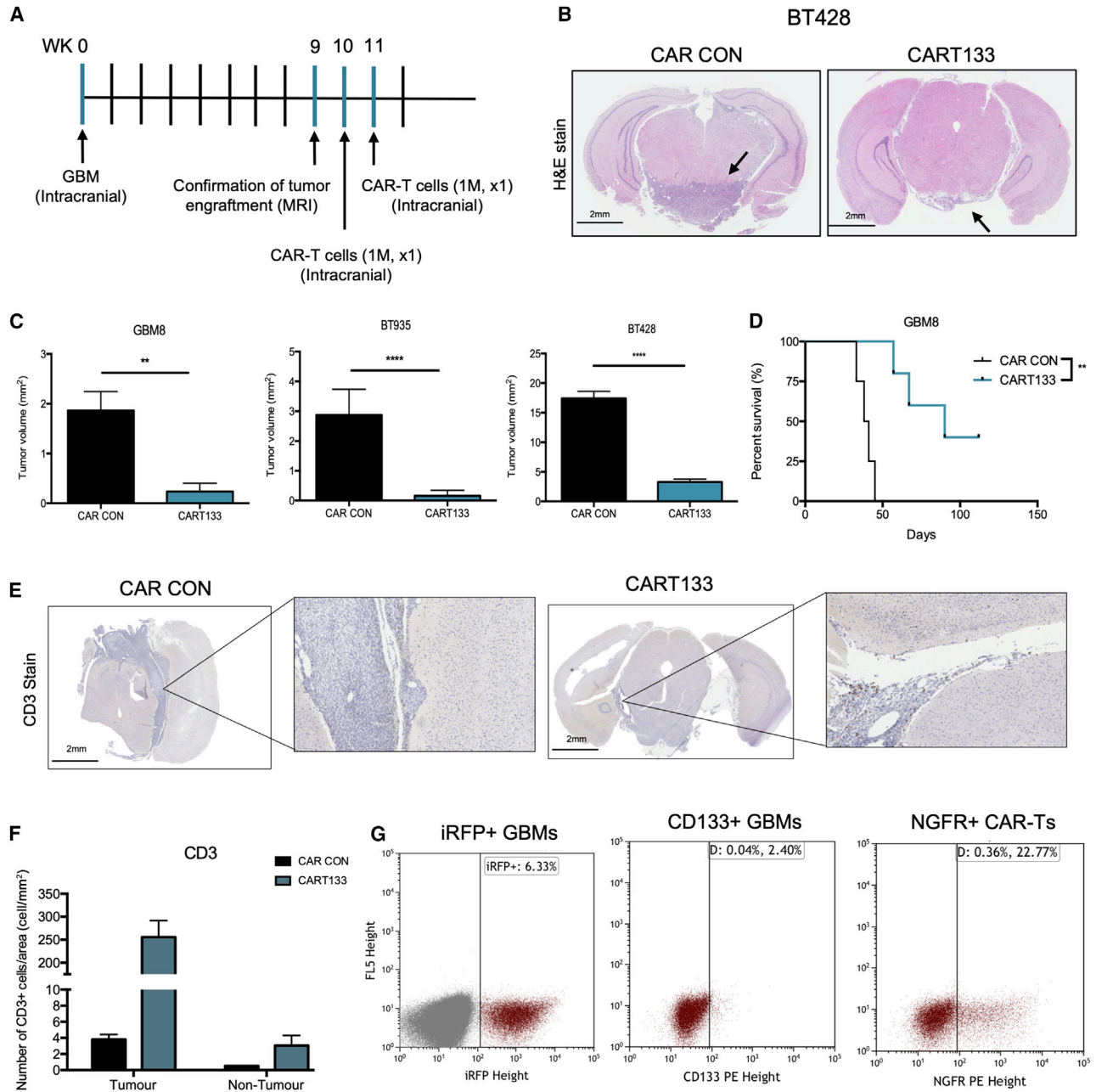
Figure 4. CART133-Mediated Antitumor Response in Xenografted Immunocompromised Mice

(A) NSG mice were intracranially implanted with human CD133^{HIGH} GBMs (1 × 10^6 cells). Upon successful engraftment, mice were intracranially treated with 1 × 10^6 CAR CON or CART133 cells once a week for 2 weeks.

(B) Mice intracranially treated with CART133 cells reveal significant elimination of tumor burden compared to control as assessed by H&E staining (n = 4).

(C and D) Mouse xenografts generated after CART133 treatment had (C) significantly less tumor masses and (D) significant survival advantage over control mice (n = 6); p = 0.0253 for BT935, and p = 0.0027 for GBM8.

(E and F) Qualitative (E) and quantitative (F) representation of CAR-T tumor infiltration and persistence at a time-matched cull post-CAR-T cell treatment.

(G) Flow-cytometric analysis of ∼1 million iRFP-expressing GBMs present in CART133-treated mice at endpoint show that only 2.40% are CD133+. Approximately 204,000 NGFR+ CAR-T cells remained in the brain at endpoint of CART133-treated mice.

models of human GBM, we sought to better define the toxicity profile of these treatments as a necessary step in the path toward clinical development. Previous studies have reported the presence of CD133+ neural stem cells in fetal brain but not from later development stages of the human brain (Uchida et al., 2000; Yu et al., 2004). Whereas the neural stem cell pool of adult patients with GBM, unlike in the developing child, is presumed to be exceedingly small and minimally functional,
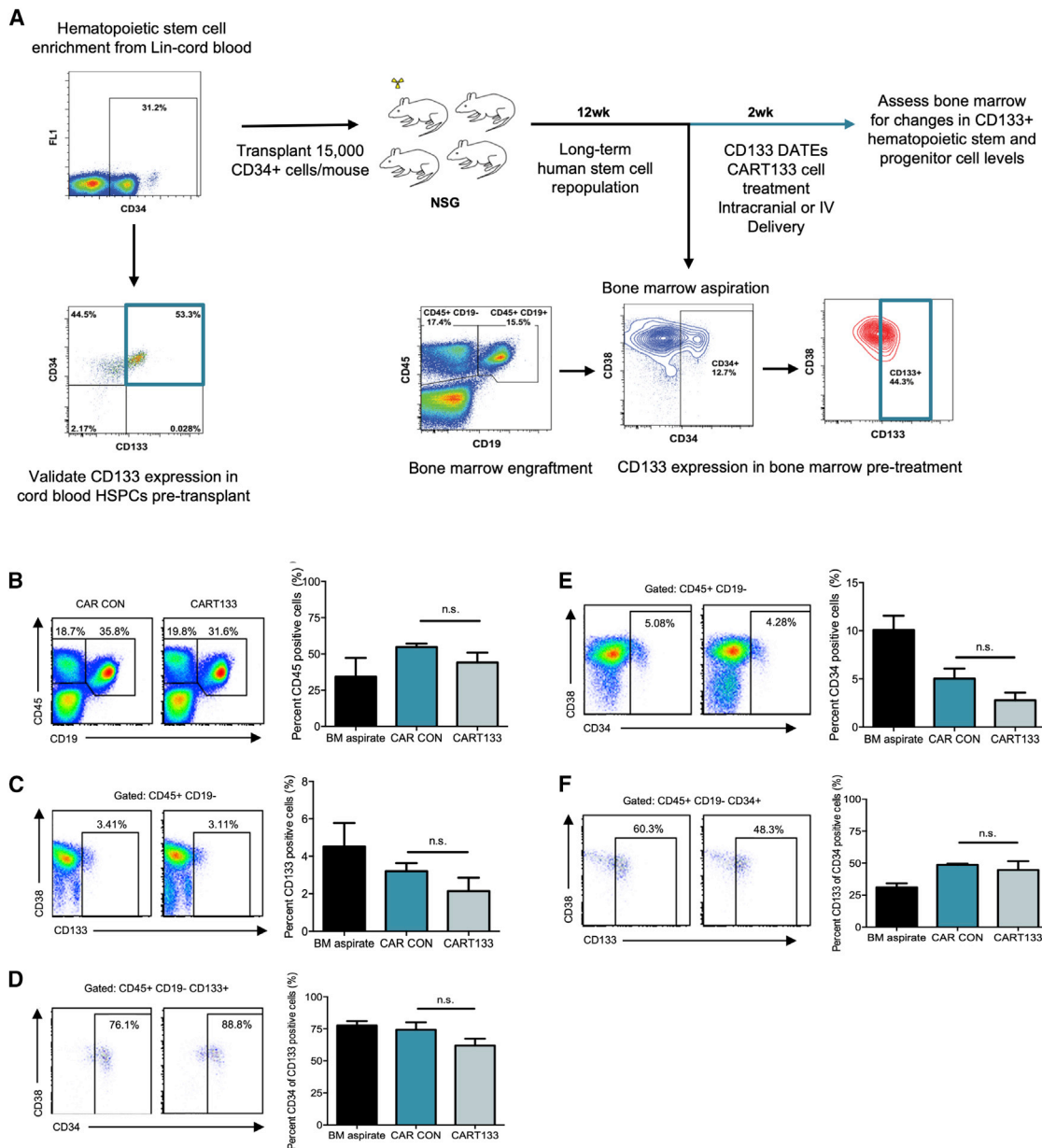
Figure 5. CD133-Targeting CAR-T Cell Treatment Does Not Significantly Reduce Numbers of Human HSPCs or Impair Hematopoiesis
(A) A schematic representation of the hematopoietic toxicity experiment.
(B) Representative flow plots and summary of levels of human hematopoietic engraftment after intracranial injection of control or CART133 cells. Treatment was performed on mice reconstituted with CD34+ CB HSPCs for 8–10 weeks. BM aspirates column indicates levels of human chimerism immediately prior to T cell therapy.
(C) Percent CD133+ BM HSPCs.
(D) Percent CD34+ cells within CD133 marked HSPCs.
(E) Percent CD34+ BM cells.
(F) Percent CD133+ HSPCs in CD34+ marked cells.

CD133+CD34+ hematopoietic stem and progenitor cells (HSPCs) (Kuçi et al., 2003; Yin et al., 1997) retain the capacity in the adult organism to engraft and differentiate to form functional hematopoietic lineages. To best of our knowledge, this is the first time that a humanized mouse model was used to test the toxicity of anti-CD133 immunotherapies against a human hematopoietic stem cell niche. Previous studies show that CD133 is not a critical regulator of HSPC function in the mouse (Arndt et al., 2013). CD133 knockout mice are viable and fertile, and they have no obvious hematopoietic defects but do exhibit retinal degeneration because of CD133's early role in retinal development and morphogenesis of photoreceptor cells (Zacchigna et al., 2009). Feasibility studies in 10 adult patients with leukemia showed that human allogeneic
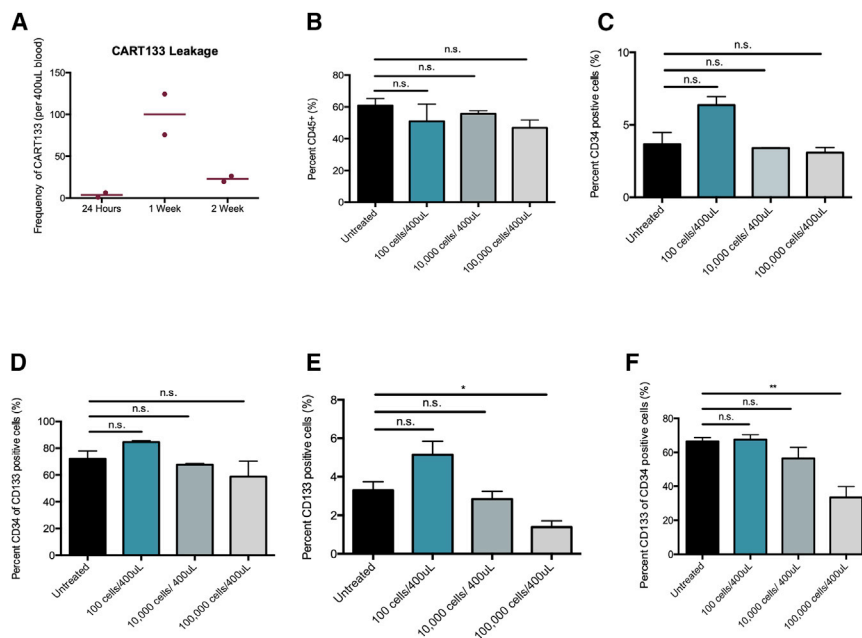
Figure 6. Intravenously Injected CD133 CAR-T Cells Do Not Significantly Reduce Numbers of Human HSPCs or Impair Hematopoiesis until Higher Doses

(A) Intracranial injections of CART133 reveal minimal leakage into the peripheral blood post-treatment. Representative summary of levels of human hematopoietic engraftment after intracranial injection of control or CARCD133 cells. Treatment was performed on mice reconstituted with CD34+ CB HSPCs for 8–10 weeks. Untreated column indicates levels of human chimerism.

(B) Percent CD45+ BM cells.

(C) Percent CD34+ BM HSPCs.

(D) Percent CD34+ cells within CD133 marked HSPCs.

(E) Percent CD133+ BM cells (Student's t test; n = 3, p = 0.0252).

(F) Percent CD133+ HSPCs in CD34+ marked cells (Student's t test; n = 3, p = 0.0082).

transplantation of CD133+ cells produced successful reconstitution of hematopoiesis in adults (Bornhäuser et al., 2005). However, whether CD133 is dispensable for the maintenance of HSPC function is unclear.

We postnatally engrafted a human hematopoietic system by injecting human fetal CD34+ cord blood (CB) cells via tail vein injections into preconditioned NSG mice. Bone marrow (BM) aspiration after 12 weeks confirmed engraftment by consistent levels of cells expressing human CD19, CD45, CD34, CD38, and CD133 (Figure 5A), after which mice were divided into two groups with the same levels of average hematopoietic graft. Mice were then treated intracranially with similar doses of either CART133 or control CAR-T cells, and BM samples were collected 2 weeks post-treatment for analysis of human HSPC chimerism. We observed no significant differences in the percentage of human CD45+ engraftments (Figure 5B). Within the human hematopoietic grafts of CAR-T-treated animals, we also detected no alteration in the levels or total numbers of CD133+ cells (Figure 5C). Furthermore, we did not observe alterations in the percentage of cells expressing the well-established marker of HSPCs, CD34, within either the CD133 compartment or the larger human grafts (Figures 5D and 5E). Finally, we explored the possibility that, within the HSPC fraction, CD133 may be differentially influenced by CAR-T injections and found, again, no alteration in its levels within these subsets (Figure 5F).

To validate the toxicity of CART133 to the hematopoietic system, we sought to treat humanized mice intravenously with increasing doses of CART133 cells. To corroborate our previous findings and establish a minimum dose for intravenous treatment, we performed leakage studies of our CART133 cells and found peak leakage (defined later) into the peripheral blood 1 week post-treatment. We treated non-tumor-bearing mice with our CART133 treatment regimen and collected peripheral blood at 24 h, 1 week, and 2 weeks post-treatment. This revealed peak leakage of CART133 into the periphery of 100 cells

per 400 μL murine blood 1 week post-treatment (Figure 6A). We subsequently intravenously treated humanized mice with 100, 10,000, or 100,000 CART133 cells per 400 μL blood. Absolute CART133 numbers were adjusted according to the estimated total blood volume for each mouse. BM samples were collected 1 week post-treatment for analysis of human HSPC chimerism to assess maximal toxicity as informed by peak leakage. We observed no significant changes in total graft as measured by CD45 positivity across all doses of CART133 compared to untreated controls (Figure 6B). In the HSPC fraction, we observed no significant differences in total BM CD34 positivity (Figure 6C) or in the CD34+ subset of CD133+ HSPCs across all conditions (Figure 6D). Additionally, CART133 treatment did not affect total CD133 positivity until the highest dose, in which there was a significant reduction (Figure 6E). This dose-dependent decrease was observed in the CD133+ subset of CD34+ cells (Figure 6F). Ultimately, we showed that, while CART133 therapy can influence total CD133 positivity in the HSPC fraction at high doses, total CD34 positivity and hematopoietic reconstitution are unaffected.

To our knowledge, the only study that systematically tested a CD133-targeted therapy on normal human CD34+ cord blood cells was a preclinical investigation of the effect of the fusion protein dCD133KDEL on head and neck cancer, where dCD133KDEL treatment showed minimal effects on normal HSPCs as assessed by long-term culture and colony-forming assays (Waldron et al., 2011). Using a dose-dependent assessment of intravenous treatment of CART133, we validated CART133's putative toxicity in the humanized mouse model. However, a significant effect on hematopoiesis was only observed at the highest dose, 100- to 1,000-fold times more than the leakage of CART133 into the peripheral blood using our intracranial dosing regimen. While the subset of CD133+ cells was significantly lower at this dose, similar to the previous report, the impact on the total CD34+ HSPCs and hematopoietic reconstitution was minimal.

Two possible explanations for these observations may be at play: (1) CD133 receptors are present in a far lower copy number in normal stem cells compared to cancer cells (Schmohl and Vallera, 2016); and (2) the human hematopoietic system is plastic, and CD133− cells have an ability to generate CD133+ cells through changes in cell state or asymmetric division, as shown in previous studies (Rutella et al., 2003) (Suuronen et al., 2006). The first explanation has been demonstrated in hepatocellular and gastric cancers (Smith et al., 2008). Specifically, in the human hematopoietic system, the number of CD133 receptors typically present on CD34-enriched normal BM progenitor cells is very low (<5,000 sites per cell) (Van Orden et al., 2007). Additional supportive evidence for our findings of the dispensable nature of human CD133+ HSPCs can be found in recently published clinical trial data (Wang et al., 2018) from a phase-I clinical trial (NCT: 02541370) of CD133 CAR-T cells for advanced metastatic malignancies conducted at the Chinese PLA General Hospital. This trial assessed the feasibility, toxicity, and efficacy of the treatment, and out of 23 patients systemically infused with $0.05–2 \times 10^{6}$/kg CD133 CAR-T cells, 3 achieved partial remission and 14 achieved stable disease. With no serious adverse events observed, the only primary toxicity was a decrease in hemoglobin, lymphocytes, and thrombocytes ($\nleqq$ grade 3), which was self-recovered within 1 week.

In summary, we present a comparative and in-depth evaluation of the preclinical efficacy and toxicity of three promising immunotherapeutic modalities directed against a novel human epitope of the most frequently used CSC surface antigen, CD133. We conclude that our CART133 cell presents a therapeutically tractable strategy to target self-renewing, chemoradioresistant, and functionally critical CD133+ BTICs that drive many cases of GBM recurrence and therapeutic resistance. CART133 therapy may also offer a feasible and effective immunotherapeutic strategy for patients with other treatment-resistant primary cancers with detectable CD133+ BTIC populations, including melanoma, ovarian cancer, lung cancer, and pancreatic cancer, as well as lung-to-brain and melanoma-to-brain metastases.

STAR★METHODS

Detailed methods are provided in the online version of this paper and include the following:

- KEY RESOURCES TABLE
- RESOURCE AVAILABILITY
  - Lead Contact
  - Materials Availability
  - Data and Code Availability
- EXPERIMENTAL MODEL AND SUBJECT DETAILS
  - Dissociation and culture of primary GBM tissue
  - Propagation of Brain tumor stem cells (BTSCs)
  - *In vivo* intracranial injections and H&E/immunostaining of xenograft tumors
  - Human umbilical cord blood stem cell enrichment and flow cytometry
  - Cord blood HSPC xenotransplantation and analysis for human chimerism
- METHOD DETAILS
  - CellectSeq Selections
  - Cell-based ELISA
  - Secondary sphere formation assay
  - Cell proliferation assay
  - Generation of CAR Lentivirus
  - Generation of CAR-T cells
  - Activation assays and Evaluation of cytokine release
  - T cell proliferation
  - Cytotoxicity assays
  - Flow cytometric analysis and sorting
  - RW03 Antibody quantification in brain tissue
- QUANTIFICATION AND STATISTICAL ANALYSIS
  - Statistical Analysis
- ADDITIONAL RESOURCES

AUTHOR CONTRIBUTIONS

P.V., C.V., J.M., and S.S. conceived and designed overall studies. R.W. performed CellectSeq studies. P.V., S.K.S., N.T., D.B., D.M., and M. Singh performed animal studies. K.H. and P.V. conceptualized humanized mouse model experiments. S.R. and N.W. generated humanized mice, and S.R., N.W., P.V., and S.K.S. performed subsequent safety studies. M.A.Q., C.C., A.D., P.V., and S.K.S. propagated brain tumor lines and performed *in vitro* assays with RW03. Flow studies were performed by N.M. and M. Subapanditha. V.H., N.T., and R.G.W. conceptualized and performed RW03 half-life experiment and data interpretation. J.P. and J.M. designed DATE constructs. P.V., C.V., J.B., and J.M. designed CAR-T constructs. P.V., C.V., S.K.S., D.U., and E.F. generated CAR-T cells for studies. P.V., C.V., S.K.S., M. Seyfrid, E.F., and N.S. performed *in vitro* characterization of DATEs and CAR-T cells. A.A.A. and S.K.S. developed and edited figures and performed statistical analyses. P.V., J.M., and S.S. drafted and edited the manuscript, with input from all authors.

REFERENCES

Anido, J., Sáez-Borderías, A., Gonzàlez-Juncà, A., Rodón, L., Folch, G., Carmona, M.A., Prieto-Sánchez, R.M., Barba, I., Martínez-Sáez, E., Prudkin, L., et al. (2010). TGF-β Receptor Inhibitors Target the CD44(high)/Id1(high) Glioma-Initiating Cell Population in Human Glioblastoma. Cancer Cell 18, 655–668.

Arndt, K., Grinenko, T., Mende, N., Reichert, D., Portz, M., Ripich, T., Carmeliet, P., Corbeil, D., and Waskow, C. (2013). CD133 is a modifier of hematopoietic progenitor frequencies but is dispensable for the maintenance of mouse hematopoietic stem cells. Proc. Natl. Acad. Sci. USA 110, 5582–5587.

Bao, S., Wu, Q., McLendon, R.E., Hao, Y., Shi, Q., Hjelmeland, A.B., Dewhirst, M.W., Bigner, D.D., and Rich, J.N. (2006). Glioma stem cells promote radioresistance by preferential activation of the DNA damage response. Nature 444, 756–760.

Bao, S., Wu, Q., Li, Z., Sathornsumetee, S., Wang, H., McLendon, R.E., Hjelmeland, A.B., and Rich, J.N. (2008). Targeting cancer stem cells through L1CAM suppresses glioma growth. Cancer Res. 68, 6043–6048.

Bobo, R.H., Laske, D.W., Akbasak, A., Morrison, P.F., Dedrick, R.L., and Oldfield, E.H. (1994). Convection-enhanced delivery of macromolecules in the brain. Proc. Natl. Acad. Sci. USA 91, 2076–2080.

Bogdahn, U., Hau, P., Stockhammer, G., Venkataramana, N.K., Mahapatra, A.K., Suri, A., Balasubramaniam, A., Nair, S., Oliushine, V., Parfenov, V., et al.; Trabedersen Glioma Study Group (2011). Targeted therapy for high-grade glioma with the TGF-β2 inhibitor trabedersen: results of a randomized and controlled phase IIb study. Neuro-oncol. 13, 132–142.

Bornhäuser, M., Eger, L., Oelschlaegel, U., Auffermann-Gretzinger, S., Kiani, A., Schetelig, J., Illmer, T., Schaich, M., Corbeil, D., Thiede, C., and Ehninger, G. (2005). Rapid reconstitution of dendritic cells after allogeneic transplantation of CD133+ selected hematopoietic stem cells. Leukemia 19, 161–165.

Brown, C.E., Badie, B., Barish, M.E., Weng, L., Ostberg, J.R., Chang, W.C., Naranjo, A., Starr, R., Wagner, J., Wright, C., et al. (2015). Bioactivity and Safety of IL13Ralpha2-Redirected Chimeric Antigen Receptor CD8+ T Cells in Patients with Recurrent Glioblastoma. Clin. Cancer Res. 21, 4062–4072.

Brown, C.E., Alizadeh, D., Starr, R., Weng, L., Wagner, J.R., Naranjo, A., Ostberg, J.R., Blanchard, M.S., Kilpatrick, J., Simpson, J., et al. (2016). Regression of Glioblastoma after Chimeric Antigen Receptor T-Cell Therapy. N. Engl. J. Med. 375, 2561–2569.

Brown, C.E., Aguilar, B., Starr, R., Yang, X., Chang, W.C., Weng, L., Chang, B., Sarkissian, A., Brito, A., Sanchez, J.F., et al. (2018). Optimization of IL13Ralpha2-Targeted Chimeric Antigen Receptor T Cells for Improved Anti-tumor Efficacy against Glioblastoma. Mol. Ther. 26, 31–44.

Burrell, R.A., McGranahan, N., Bartek, J., and Swanton, C. (2013). The causes and consequences of genetic heterogeneity in cancer evolution. Nature 501, 338–345.

Chen, J., Li, Y., Yu, T.S., McKay, R.M., Burns, D.K., Kernie, S.G., and Parada, L.F. (2012). A restricted cell population propagates glioblastoma growth after chemotherapy. Nature 488, 522–526.

Chen, Y.-L., Lin, P.-Y., Ming, Y.-Z., Huang, W.-C., Chen, R.-F., Chen, P.-M., and Chu, P.-Y. (2017). The effects of the location of cancer stem cell marker CD133 on the prognosis of hepatocellular carcinoma patients. BMC Cancer 17, 474.

Choi, B.D., Gedeon, P.C., Sanchez-Perez, L., Bigner, D.D., and Sampson, J.H. (2013). Regulatory T cells are redirected to kill glioblastoma by an EGFRvIII-targeted bispecific antibody. OncoImmunology 2, e26757.

Corbin, A.S., Agarwal, A., Loriaux, M., Cortes, J., Deininger, M.W., and Druker, B.J. (2011). Human chronic myeloid leukemia stem cells are insensitive to imatinib despite inhibition of BCR-ABL activity. J. Clin. Invest. 121, 396–409.

Cox, C.V., Diamanti, P., Evely, R.S., Kearns, P.R., and Blair, A. (2009). Expression of CD133 on leukemia-initiating cells in childhood ALL. Blood 113, 3287–3296.

Diehn, M., Cho, R.W., Lobo, N.A., Kalisky, T., Dorie, M.J., Kulp, A.N., Qian, D., Lam, J.S., Ailles, L.E., Wong, M., et al. (2009). Association of reactive oxygen species levels and radioresistance in cancer stem cells. Nature 458, 780–783.

Ding, D., Kanaly, C.W., Bigner, D.D., Cummings, T.J., Herndon, J.E., 2nd, Pastan, I., Raghavan, R., and Sampson, J.H. (2010a). Convection-enhanced delivery of free gadolinium with the recombinant immunotoxin MR1-1. J. Neurooncol. 98, 1–7.

Ding, D., Kanaly, C.W., Cummings, T.J., Herndon, J.E., 2nd, Raghavan, R., and Sampson, J.H. (2010b). Long-term safety of combined intracerebral delivery of free gadolinium and targeted chemotherapeutic agent PRX321. Neurol. Res. 32, 810–815.

Dylla, S.J., Beviglia, L., Park, I.K., Chartier, C., Raval, J., Ngan, L., Pickell, K., Aguilar, J., Lazetic, S., Smith-Berdan, S., et al. (2008). Colorectal cancer stem cells are enriched in xenogeneic tumors following chemotherapy. PLoS ONE 3, e2428.

Hammill, J.A., VanSeggelen, H., Helsen, C.W., Denisova, G.F., Evelegh, C., Tantalo, D.G., Bassett, J.D., and Bramson, J.L. (2015). Designed ankyrin repeat proteins are effective targeting elements for chimeric antigen receptors. J. Immunother. Cancer 3, 55.

Han, M., Guo, L., Zhang, Y., Huang, B., Chen, A., Chen, W., Liu, X., Sun, S., Wang, K., Liu, A., and Li, X. (2016). Clinicopathological and Prognostic Significance of CD133 in Glioma Patients: A Meta-Analysis. Mol. Neurobiol. 53, 720–727.

Hermann, P.C., Huber, S.L., Herrler, T., Aicher, A., Ellwart, J.W., Guba, M., Bruns, C.J., and Heeschen, C. (2007). Distinct populations of cancer stem cells determine tumor growth and metastatic activity in human pancreatic cancer. Cell Stem Cell 1, 313–323.

Karbanová, J., Missol-Kolka, E., Fonseca, A.V., Lorra, C., Janich, P., Hollerová, H., Jászai, J., Ehrmann, J., Kolář, Z., Liebers, C., et al. (2008). The stem cell marker CD133 (Prominin-1) is expressed in various human glandular epithelia. J. Histochem. Cytochem. 56, 977–993.

Kreso, A., van Galen, P., Pedley, N.M., Lima-Fernandes, E., Frelin, C., Davis, T., Cao, L., Baiazitov, R., Du, W., Sydorenko, N., et al. (2014). Self-renewal as a therapeutic target in human colorectal cancer. Nat. Med. 20, 29–36.

Kuçi, S., Wessels, J.T., Bühring, H.J., Schilbach, K., Schumm, M., Seitz, G., Löffler, J., Bader, P., Schlegel, P.G., Niethammer, D., and Handgretinger, R. (2003). Identification of a novel class of human adherent CD34- stem cells that give rise to SCID-repopulating cells. Blood 101, 869–876.

Lai, H., and Singh, N.P. (2004). Magnetic-field-induced DNA strand breaks in brain cells of the rat. Environ. Health Perspect. 112, 687–694.

Lathia, J.D., Gallagher, J., Heddleston, J.M., Wang, J., Eyler, C.E., Macswords, J., Wu, Q., Vasanji, A., McLendon, R.E., Hjelmeland, A.B., and Rich, J.N. (2010). Integrin alpha 6 regulates glioblastoma stem cells. Cell Stem Cell 6, 421–432.

Leong, K.G., Wang, B.E., Johnson, L., and Gao, W.Q. (2008). Generation of a prostate from a single adult stem cell. Nature 456, 804–808.

Li, B., McCrudden, C.M., Yuen, H.F., Xi, X., Lyu, P., Chan, K.W., Zhang, S.D., and Kwok, H.F. (2017). CD133 in brain tumor: the prognostic factor. Oncotarget 8, 11144–11159.

Liu, G., Yuan, X., Zeng, Z., Tunici, P., Ng, H., Abdulkadir, I.R., Lu, L., Irvin, D., Black, K.L., and Yu, J.S. (2006). Analysis of gene expression and chemoresistance of CD133+ cancer stem cells in glioblastoma. Mol. Cancer 5, 67.

Mak, A.B., Blakely, K.M., Williams, R.A., Penttilä, P.A., Shukalyuk, A.I., Osman, K.T., Kasimer, D., Ketela, T., and Moffat, J. (2011). CD133 protein N-glycosylation processing contributes to cell surface recognition of the primitive cell marker AC133 epitope. J. Biol. Chem. 286, 41046–41056.

Mak, A.B., Nixon, A.M., Kittanakom, S., Stewart, J.M., Chen, G.I., Curak, J., Gingras, A.C., Mazitschek, R., Neel, B.G., Stagljar, I., and Moffat, J. (2012). Regulation of CD133 by HDAC6 promotes β-catenin signaling to suppress cancer cell differentiation. Cell Rep. 2, 951–963.

Meacham, C.E., and Morrison, S.J. (2013). Tumour heterogeneity and cancer cell plasticity. Nature 501, 328–337.

Meyer, M., Reimand, J., Lan, X., Head, R., Zhu, X., Kushida, M., Bayani, J., Pressey, J.C., Lionel, A.C., Clarke, I.D., et al. (2015). Single cell-derived clonal

analysis of human glioblastoma links functional and genomic heterogeneity. Proc. Natl. Acad. Sci. USA *112*, 851–856.

Nixon, A.M.L., Duque, A., Yelle, N., McLaughlin, M., Davoudi, S., Pedley, N.M., Haynes, J., Brown, K.R., Pan, J., Hart, T., et al. (2019). A rapid in vitro methodology for simultaneous target discovery and antibody generation against functional cell subpopulations. Sci. Rep. *9*, 842.

O'Brien, C.A., Pollett, A., Gallinger, S., and Dick, J.E. (2007). A human colon cancer cell capable of initiating tumour growth in immunodeficient mice. Nature *445*, 106–110.

O'Hear, C., and Foote, J. (2006). Antibody buffering in the brain. J. Mol. Biol. *364*, 1003–1009.

O'Rourke, D.M., Nasrallah, M.P., Desai, A., Melenhorst, J.J., Mansfield, K., Morrissette, J.J.D., Martinez-Lage, M., Brem, S., Maloney, E., Shen, A., et al. (2017). A single dose of peripherally infused EGFRvIII-directed CAR T cells mediates antigen loss and induces adaptive resistance in patients with recurrent glioblastoma. Sci. Transl. Med. *9*, eaaa0984.

Oravecz-Wilson, K.I., Philips, S.T., Yilmaz, O.H., Ames, H.M., Li, L., Crawford, B.D., Gauvin, A.M., Lucas, P.C., Sitwala, K., Downing, J.R., et al. (2009). Persistence of leukemia-initiating cells in a conditional knockin model of an imatinib-responsive myeloproliferative disorder. Cancer Cell *16*, 137–148.

Patel, A.P., Tirosh, I., Trombetta, J.J., Shalek, A.K., Gillespie, S.M., Wakimoto, H., Cahill, D.P., Nahed, B.V., Curry, W.T., Martuza, R.L., et al. (2014). Single-cell RNA-seq highlights intratumoral heterogeneity in primary glioblastoma. Science *344*, 1396–1401.

Patrizii, M., Bartucci, M., Pine, S.R., and Sabaawy, H.E. (2018). Utility of Glioblastoma Patient-Derived Orthotopic Xenografts in Drug Discovery and Personalized Therapy. Front. Oncol. *8*, 23.

Persson, H., Ye, W., Wernimont, A., Adams, J.J., Koide, A., Koide, S., Lam, R., and Sidhu, S.S. (2013). CDR-H3 diversity is not required for antigen recognition by synthetic antibodies. J. Mol. Biol. *425*, 803–811.

Prasad, S., Gaedicke, S., Machein, M., Mittler, G., Braun, F., Hettich, M., Firat, E., Klingner, K., Schüler, J., Wider, D., et al. (2015). Effective Eradication of Glioblastoma Stem Cells by Local Application of an AC133/CD133-Specific T-cell-Engaging Antibody and CD8 T Cells. Cancer Res. *75*, 2166–2176.

Priceman, S.J., Tilakawardane, D., Jeang, B., Aguilar, B., Murad, J.P., Park, A.K., Chang, W.C., Ostberg, J.R., Neman, J., Jandial, R., et al. (2018). Regional Delivery of Chimeric Antigen Receptor-Engineered T Cells Effectively Targets HER2+ Breast Cancer Metastasis to the Brain. Clin. Cancer Res. *24*, 95–105.

Rudnick, J.D., Fink, K.L., Landolfi, J.C., Markert, J., Piccioni, D.E., Glantz, M.J., Swanson, S.J., Gringeri, A., and Yu, J. (2017). Immunological targeting of CD133 in recurrent glioblastoma: A multi-center phase I translational and clinical study of autologous CD133 dendritic cell immunotherapy. J. Clin. Oncol. *35*, 2059.

Rutella, S., Bonanno, G., Marone, M., De Ritis, D., Mariotti, A., Voso, M.T., Scambia, G., Mancuso, S., Leone, G., and Pierelli, L. (2003). Identification of a novel subpopulation of human cord blood CD34-CD133-CD7-CD45+lineage- cells capable of lymphoid/NK cell differentiation after in vitro exposure to IL-15. J. Immunol. *171*, 2977–2988.

Sachlos, E., Risueño, R.M., Laronde, S., Shapovalova, Z., Lee, J.H., Russell, J., Malig, M., McNicol, J.D., Fiebig-Comyn, A., Graham, M., et al. (2012). Identification of drugs including a dopamine receptor antagonist that selectively target cancer stem cells. Cell *149*, 1284–1297.

Sagrinati, C., Netti, G.S., Mazzinghi, B., Lazzeri, E., Liotta, F., Frosali, F., Ronconi, E., Meini, C., Gacci, M., Squecco, R., et al. (2006). Isolation and characterization of multipotent progenitor cells from the Bowman's capsule of adult human kidneys. J. Am. Soc. Nephrol. *17*, 2443–2456.

Schmohl, J.U., and Vallera, D.A. (2016). CD133, Selectively Targeting the Root of Cancer. Toxins (Basel) *8*, E165.

Schmohl, J.U., Felices, M., Todhunter, D., Taras, E., Miller, J.S., and Vallera, D.A. (2016a). Tetraspecific scFv construct provides NK cell mediated ADCC and self-sustaining stimuli via insertion of IL-15 as a cross-linker. Oncotarget *7*, 73830–73844.

Schmohl, J.U., Gleason, M.K., Dougherty, P.R., Miller, J.S., and Vallera, D.A. (2016b). Heterodimeric Bispecific Single Chain Variable Fragments (scFv) Killer Engagers (BiKEs) Enhance NK-cell Activity Against CD133+ Colorectal Cancer Cells. Target. Oncol. *11*, 353–361.

Shibahara, I., Sonoda, Y., Saito, R., Kanamori, M., Yamashita, Y., Kumabe, T., Watanabe, M., Suzuki, H., Watanabe, T., Ishioka, C., and Tominaga, T. (2013). The expression status of CD133 is associated with the pattern and timing of primary glioblastoma recurrence. Neuro Oncol. *15*, 1151–1159.

Shiheido, H., Chen, C., Hikida, M., Watanabe, T., and Shimizu, J. (2014). Modulation of the human T cell response by a novel non-mitogenic anti-CD3 antibody. PLoS ONE *9*, e94324.

Shlush, L.I., Zandi, S., Mitchell, A., Chen, W.C., Brandwein, J.M., Gupta, V., Kennedy, J.A., Schimmer, A.D., Schuh, A.C., Yee, K.W., et al.; HALT Pan-Leukemia Gene Panel Consortium (2014). Identification of pre-leukaemic haematopoietic stem cells in acute leukaemia. Nature *506*, 328–333.

Singh, S.K., Clarke, I.D., Terasaki, M., Bonn, V.E., Hawkins, C., Squire, J., and Dirks, P.B. (2003). Identification of a cancer stem cell in human brain tumors. Cancer Res. *63*, 5821–5828.

Singh, S.K., Hawkins, C., Clarke, I.D., Squire, J.A., Bayani, J., Hide, T., Henkelman, R.M., Cusimano, M.D., and Dirks, P.B. (2004). Identification of human brain tumour initiating cells. Nature *432*, 396–401.

Skorzewska, A., Lal, S., Waserman, J., and Guyda, H. (1989). Abnormal food-seeking behavior after surgery for craniopharyngioma. Neuropsychobiology *21*, 17–20.

Smith, L.M., Nesterova, A., Ryan, M.C., Duniho, S., Jonas, M., Anderson, M., Zabinski, R.F., Sutherland, M.K., Gerber, H.P., Van Orden, K.L., et al. (2008). CD133/prominin-1 is a potential therapeutic target for antibody-drug conjugates in hepatocellular and gastric cancers. Br. J. Cancer *99*, 100–109.

Son, M.J., Woolard, K., Nam, D.H., Lee, J., and Fine, H.A. (2009). SSEA-1 is an enrichment marker for tumor-initiating cells in human glioblastoma. Cell Stem Cell *4*, 440–452.

Suuronen, E.J., Wong, S., Kapila, V., Waghray, G., Whitman, S.C., Mesana, T.G., and Ruel, M. (2006). Generation of CD133+ cells from CD133- peripheral blood mononuclear cells and their properties. Cardiovasc. Res. *70*, 126–135.

Suvà, M.L., Rheinbay, E., Gillespie, S.M., Patel, A.P., Wakimoto, H., Rabkin, S.D., Riggi, N., Chi, A.S., Cahill, D.P., Nahed, B.V., et al. (2014). Reconstructing and reprogramming the tumor-propagating potential of glioblastoma stem-like cells. Cell *157*, 580–594.

Swanton, C. (2015). Cancer evolution constrained by mutation order. N. Engl. J. Med. *372*, 661–663.

Uchida, N., Buck, D.W., He, D., Reitsma, M.J., Masek, M., Phan, T.V., Tsukamoto, A.S., Gage, F.H., and Weissman, I.L. (2000). Direct isolation of human central nervous system stem cells. Proc. Natl. Acad. Sci. USA *97*, 14720–14725.

Van Orden, K., Birse, C., He, T., Smith, L., McKinnon, K., Lee, C., FitzHugh, W., Duniho, S., Nesterova, A., McCaffery, I., et al. (2007). Proteomic analysis of colorectal tumor cells identifies CD133/Prominin-1, a cancer stem cell marker, as a monoclonal antibody therapeutic candidate. Cancer Res. *67* (9, Suppl.), 1324.

VanSeggelen, H., Hammill, J.A., Dvorkin-Gheva, A., Tantalo, D.G., Kwiecien, J.M., Denisova, G.F., Rabinovich, B., Wan, Y., and Bramson, J.L. (2015). T Cells Engineered With Chimeric Antigen Receptors Targeting NKG2D Ligands Display Lethal Toxicity in Mice. Mol. Ther. *23*, 1600–1610.

Venugopal, C., Li, N., Wang, X., Manoranjan, B., Hawkins, C., Gunnarsson, T., Hollenberg, R., Klurfan, P., Murty, N., Kwiecien, J., et al. (2012). Bmi1 marks intermediate precursors during differentiation of human brain tumor initiating cells. Stem Cell Res. (Amst.) *8*, 141–153.

Venugopal, C., Hallett, R., Vora, P., Manoranjan, B., Mahendram, S., Qazi, M.A., McFarlane, N., Subapanditha, M., Nolte, S.M., Singh, M., et al. (2015). Pyrvinium Targets CD133 in Human Glioblastoma Brain Tumor-Initiating Cells. Clin. Cancer Res. *21*, 5324–5337.

Waldron, N.N., Kaufman, D.S., Oh, S., Inde, Z., Hexum, M.K., Ohlfest, J.R., and Vallera, D.A. (2011). Targeting tumor-initiating cancer cells with dCD133KDEL

shows impressive tumor reductions in a xenotransplant model of human head and neck cancer. Mol. Cancer Ther. *10*, 1829–1838.

Waldron, N.N., Barsky, S.H., Dougherty, P.R., and Vallera, D.A. (2014). A bispecific EpCAM/CD133-targeted toxin is effective against carcinoma. Target. Oncol. *9*, 239–249.

Wang, Y., Chen, M., Wu, Z., Tong, C., Dai, H., Guo, Y., Liu, Y., Huang, J., Lv, H., Luo, C., et al. (2018). CD133-directed CAR T cells for advanced metastasis malignancies: A phase I trial. OncoImmunology *7*, e1440169.

Wei, Y., Jiang, Y., Zou, F., Liu, Y., Wang, S., Xu, N., Xu, W., Cui, C., Xing, Y., Liu, Y., et al. (2013). Activation of PI3K/Akt pathway by CD133-p85 interaction promotes tumorigenic capacity of glioma stem cells. Proc. Natl. Acad. Sci. USA *110*, 6829–6834.

Wolak, D.J., Pizzo, M.E., and Thorne, R.G. (2015). Probing the extracellular diffusion of antibodies in brain using in vivo integrative optical imaging and ex vivo fluorescence imaging. J. Control. Release *197*, 78–86.

Yin, A.H., Miraglia, S., Zanjani, E.D., Almeida-Porada, G., Ogawa, M., Leary, A.G., Olweus, J., Kearney, J., and Buck, D.W. (1997). AC133, a novel marker for human hematopoietic stem and progenitor cells. Blood *90*, 5002–5012.

Yu, S., Zhang, J.Z., Zhao, C.L., Zhang, H.Y., and Xu, Q. (2004). Isolation and characterization of the CD133+ precursors from the ventricular zone of human fetal brain by magnetic affinity cell sorting. Biotechnol. Lett. *26*, 1131–1136.

Zacchigna, S., Oh, H., Wilsch-Bräuninger, M., Missol-Kolka, E., Jászai, J., Jansen, S., Tanimoto, N., Tonagel, F., Seeliger, M., Huttner, W.B., et al. (2009). Loss of the cholesterol-binding protein prominin-1/CD133 causes disk dysmorphogenesis and photoreceptor degeneration. J. Neurosci. *29*, 2297–2308.

Zeppernick, F., Ahmadi, R., Campos, B., Dictus, C., Helmke, B.M., Becker, N., Lichter, P., Unterberg, A., Radlwimmer, B., and Herold-Mende, C.C. (2008). Stem cell marker CD133 affects clinical outcome in glioma patients. Clin. Cancer Res. *14*, 123–129.

Zhang, J., Guo, X., Chang, D.Y., Rosen, D.G., Mercado-Uribe, I., and Liu, J. (2012). CD133 expression associated with poor prognosis in ovarian cancer. Mod. Pathol. *25*, 456–464.

Zhu, Z., Khan, M.A., Weiler, M., Blaes, J., Jestaedt, L., Geibert, M., Zou, P., Gronych, J., Bernhardt, O., Korshunov, A., et al. (2014). Targeting self-renewal in high-grade brain tumors leads to loss of brain tumor stem cells and prolonged survival. Cell Stem Cell *15*, 185–198.

Zhu, X., Prasad, S., Gaedicke, S., Hettich, M., Firat, E., and Niedermann, G. (2015). Patient-derived glioblastoma stem cells are killed by CD133-specific CAR T cells but induce the T cell aging marker CD57. Oncotarget *6*, 171–184.

STAR★METHODS

KEY RESOURCES TABLE

REAGENT or RESOURCE	SOURCE	IDENTIFIER
Antibodies		
RW03	This manuscript	N/A
CD133/2-APC	Miltenyi Biotec	Cat#130-112-158, RRID:AB_2654902
CD3-PECy7	BD Biosciences	Cat#557851, RRID:AB_396896
CD25-FITC	Miltenyi Biotec	Cat#130-113-283, RRID:AB_2734062
CD69-APC	BD Biosciences	Cat#555533, RRID:AB_398602
NGFR-PE	Miltenyi Biotec	Cat#130-112-790, RRID:AB_2725887
Myc-FITC	Miltenyi Biotec	Cat#130-116-653, RRID:AB_275132
M13-HRP	Abcam	Cat#50370, RRID:AB_881599
Goat Anti-Human IgG AF488, F(ab')2 fragment specific	Jackson ImmunoResearch	Cat#109-546-097, RRID:AB_2337849
Goat Anti-Human IgG, F(ab')2 fragment specific	Jackson ImmunoResearch	Cat#109-005-006, RRID: AB_2337533
CD45-BV421	Thermo Fischer Scientific	Cat#MHCD4528, RRID:AB_10375161
CD34-FITC	BD Biosciences	Cat#555821, RRID:AB_396150
CD33-PE	BD Biosciences	Cat#347787, RRID:AB_400350
CD19-APC	BD Biosciences	Cat#555415, RRID:AB_398597
CD38-PECy7	BD Biosciences	Cat#335790, RRID:AB_399969
Mouse Fc block	BD Biosciences	Cat#553142
Human IgG	Millipore Sigma	Cat#I4506
IgG Compbeads	BD Biosciences	Cat#552843
Chemicals, Peptides, and Recombinant Proteins		
7AAD Viability dye	Beckman Coulter	Cat#A07704
Liberase Blendzyme 3	Millipore Sigma	Cat#5401119001
Ammonium Chloride	STEMCELL Technologies	Cat#07850
NeuroCult NS-A Proliferation Kit (Human)	STEMCELL Technologies	Cat#05751
Heparin Solution	STEMCELL Technologies	Cat#07980
Human Recombinant Basic Fibroblast Growth Factor (bFGF)	STEMCELL Technologies	Cat#78003
Human Recombinant Epidermal Growth Factor (EGF)	STEMCELL Technologies	Cat#78006
Antibiotic-Antimycotic (100X)	Wisent Bioproducts	Cat#450-115-EL
Lipofectamine 3000	ThermoFisher	Cat#L3000075
Fetal Bovine Serum, heat inactivated (FBS)	Wisent	Cat#098-150
PBS	ThermoFisher	Cat#10010049
DMEM	ThermoFisher	Cat#11995073
HEPES	ThermoFisher	Cat#15630080
EDTA	Millipore Sigma	Cat#20158
NaCL	Millipore Sigma	Cat#5886
HCL	Millipore Sigma	Cat#
Sodium Bicarbonate	Millipore Sigma	Cat#S5761
D-Glucose	Millipore Sigma	Cat#G7021
KCl	Millipore Sigma	Cat#60142
2x YT Culture Medium	Millipore Sigma	Cat#Y2377-250G
Polyethylene Glycol (PEG)	Sigma-Aldrich	Cat#P1458
Paraformaldehyde	Electron Microscopy Biosciences	Cat#RT15700
TMB Peroxidase substrate and Peroxidase substrate solution B (KPL)	ThermoFisher	Cat#N301

Continued

REAGENT or RESOURCE	SOURCE	IDENTIFIER
XSFM Media	Irvine Scientific	Cat#91141
Recombinant human interleukin 7 (rh-1L7)	Peprotech	Cat#200-07
Recombinant human interleukin 2 (rh-1L2)	Peprotech	Cat#200-02
PrestoBlue	ThermoFisher	Cat#A13262
D-firefly luciferin potassium salt	Perkin Elmer	Cat#122799
Nonidet 40 (NP40)	ThermoFisher	Cat#98379
Ficoll-Paque Plus	GE Healthcare	Cat#17144003
Ammonium Chloride Solution	STEMCELL Technologies	Cat#07800
Cy7-sulfo-NHS ester	Lumiprobe	Cat#15320
Glycerol	Millipore Sigma	Cat#G5516
Critical Commercial Assays		
EasySep Human Progenitor Cell Enrichment Kit	STEMCELL Technologies	Cat#19356
Cytometric Bead Array (CBA) Kit	BD Biosciences	Cat#550749
SepMate	STEMCELL Technologies	Cat#85450
Libraries and Data Sets		
Fab Phage Library F	Persson et al., 2013	N/A
Software		
GraphPad Prism 5.0	GraphPad Software Inc.	https://www.graphpad.com/scientific-software/prism/
FlowJo	FLOWJO LLC	https://www.flowjo.com/
BD FACSDiva	BD Biosciences	https://www.bdbiosciences.com/en-us/instruments/research-instruments/research-software/flow-cytometry-acquisition/facsdiva-software
Tecan Infinite M200 Pro		N/A
Aperio ScanScope	Leica Biosystems	N/A
FLUOstar Omega Fluorescence 556 Microplate reader	BMG labtech	N/A
Recombinant DNA		
CART133 Lentiviral Constructs	This manuscript	N/A
CAR CON Lentiviral Constructs		N/A
PMD2.G	Addgene	RRID:Addgene_12259
psPAX	Addgene	RRID:Addgene_12260
Firefly Luciferase	Addgene	RRID:Addgene_118017
Experimental Models: Cell Lines		
GBM8	Massachusetts General Hospital, Dr. Hiroaki Wakimoto	N/A
Patient-derived human GBM lines	This manuscript	See Table S1
Bacterial Strains		
XLI-Blue Competent Cells	Agilent Technologies	Cat#200249
MI3K07 Helper Phage	ThermoFisher	Cat#18311019
Experimental Models: Organisms/Strains		
NOD-scid IL2Rgammanull (NSG) Mouse	Jackson Laboratory	Stock # 005557
Other		
Dialysis Membrane	Spectrapor	Cat#08-667A
10 μl Hamilton syringe	Hamilton	Cat#76350-01
100 mm Ultra-Low Attachment Culture Dish	Corning	Cat#431110
70μm Cell strainer	Falcon	Cat#08-771-2
96 well dish	Gernier	Cat#655970
CD3/CD28 Dynabeads	GIBCO	Cat#113.31D

RESOURCE AVAILABILITY

Lead Contact
Further information and requests for resources and reagents should be directed to and will be fulfilled by the Lead Contact, Dr. Sheila Singh, ssingh@mcmaster.ca.

Materials Availability
- There are restrictions to the availability of the CD133-binding agents (RW03 scFv) and uses thereof for treating cancer due to patents. (Patent No. 2,966,157; No. 2017800782373; No. EP17863201; No. 2019-521046; No. 16/342,807).
- In-house generated recombinant DNA for generation of DATEs and CAR-Ts, and patient-derived tissues (Table S1) can be provided for collaborative research under Material Transfer Agreement (MTA) with Singh lab/McMaster University.
- The phage-displayed synthetic antibody fragment (Fab) Library F can be provided for collaborative research under Material Transfer Agreement (MTA) with Moffat lab/University of Toronto.

Data and Code Availability
- The CD133 tissue expression and survival in Figures S1B and S1C were taken from The Cancer Genome Atlas Adult GBM RNA-seq data, https://gliovis.shinyapps.io/GlioVis/
- This study did not generate any unique datasets or code.

EXPERIMENTAL MODEL AND SUBJECT DETAILS

Dissociation and culture of primary GBM tissue
Human GBM samples (Table S1) were obtained from consenting patients, as approved by the Hamilton Health Sciences/McMaster Health Sciences Research Ethics Board. Brain tumor samples were dissociated in PBS (ThermoFisher, Cat#10010049) containing 0.2 Wünsch unit/mL Liberase Blendzyme 3 (Millipore Sigma, Cat#5401119001), and incubated in a shaker at 37°C for 15 min. The dissociated tissue was filtered through a 70μm cell strainer (Falcon, Cat#08-771-2) and collected by centrifugation (1500 rpm, 3 min). Red blood cells were lysed using ammonium chloride solution (STEMCELL Technologies, Cat#07850). GBM cells were resuspended in Neurocult complete (NCC) media, a chemically defined serum-free neural stem cell medium (STEMCELL Technologies, Cat#05751), supplemented with human recombinant epidermal growth factor (20ng/mL: STEMCELL Technologies, Cat#78006), basic fibroblast growth factor (20ng/mL; STEMCELL Technologies Cat#78006), heparin (2 μg/mL 0.2% Heparin Sodium Salt in PBS; STEMCELL technologies, Cat#07980), antibiotic-antimycotic (1X; Wisent, Cat# 450-115-EL), and plated on ultra-low attachment plates (Corning, Cat#431110) and cultured as neurospheres. GBM8 was a kind gift from Dr. Hiroaki Wakimoto (Massachusetts General Hospital, Boston, MA, USA).

Propagation of Brain tumor stem cells (BTSCs)
Neurospheres derived from minimally-cultured (< 20 passages) human GBM samples were plated on polyornithine- laminin coated plates for adherent growth. Adherent cells were replated in low-binding plates and cultured as tumorspheres, which were maintained as spheres upon serial passaging *in vitro*. As shown before, compared to commercially available GBM cell lines, patient derived 3D cultures represent the variety of heterogeneous clones present within patient samples (Patrizii et al., 2018). These models recapitulate the key GBM morphological, architectural and expression features that are present in primary GBM. These cells retained their self-renewal potential and were capable of *in vivo* tumor formation.

In vivo intracranial injections and H&E/immunostaining of xenograft tumors
Animal studies were performed according to guidelines under Animal Use Protocols of McMaster University Central Animal Facility. Intracranial injections in 6-8 week old NSG mice were performed as previously described (Singh et al., 2004) using each of the following GBMs: GBM cells (1e^6 BT935, 250,000 GBM8 and 1M BT428). Briefly, a burr hole is drilled at the point located 2 mm behind the coronal suture, and 3 mm to the right of the sagittal suture and GBM cells suspended in 10 μL PBS are intracranially injected with a Hamilton syringe (Hamilton, Cat#7635-01) into right frontal lobes of 6-8 week old NSG mice. For RW03-IgG treatment, RW03 IgG or control IgG injections were started after half-maximal tumor engraftment and continued for twice a week for two weeks. For DATE treatment, mice were treated with 50μg of DATE with 1e^6 PBMCs by intracranial injections twice a week for two weeks. For CAR-T treatment, 1e^6 CAR-Control or CAR-CD133 T cells were injected twice a week for two weeks. For tumor volume evaluation, animals were sacrificed when control mice reached endpoint. When mice reached endpoint, they were perfused with 10% formalin and collected brains were sliced at 2mm thickness using brain-slicing matrix for paraffin embedding and H&E staining or CD3 staining for CAR-Ts. Images were captured using an Aperio Slide Scanner (Leica Biosystems) and analyzed using ImageScope v11.1.2.760 software (Aperio). For survival studies, all the mice were kept until they reached endpoint and number of days of survival were noted for *Kaplan Meyer* Analysis. CD3 stained slides were scanned and captured using an Aperio Slide Scanner and analyzed

using ImageScope v11.1.2.760 software (Aperio). Tumor area and number of CD3 positive cells were generated using Aperio Membrane Algorithm, and reported as number of CD3 positive cells per area (mm^2).

Human umbilical cord blood stem cell enrichment and flow cytometry

Cord blood samples were obtained with informed patient consent by Trillium Health Partners in accordance with Research Ethics Board approval. Cord blood mononuclear cells were collected by centrifugation with Ficoll-Paque Plus (GE Healthcare, Cat#17144003) and red blood cell lysis with ammonium chloride (StemCell Technologies, Inc., Cat#07800). Cord blood HSPCs were enriched with the EasySep Human Progenitor Cell Enrichment Kit with Platelet Depletion (StemCell Technologies, Inc., Cat#19356). Cryopreserved lineage negative HSPCs were used for all hematopoietic reconstitution experiments.

Cord blood HSPC xenotransplantation and analysis for human chimerism

To perform human HSPC xenotransplants, Lin- samples were pooled and HSPCs enriched by sorting on CD34 marker expression. 15,000-18,000 CD34+ cells were injected per sublethally irradiated (315 cGy) NSG mouse *via* tail vein. Injected mice were analyzed for human hematopoietic engraftment at 8-10 weeks post transplantation by femoral bone marrow aspiration. Mice engrafted at > 5% human CD45+ in aspirated bone marrow were used for subsequent intracranial injections with anti-CD133 antibody therapy, CAR-T cell, or DATEs. Analysis of human hematopoietic chimerism after immunotherapy treatment was performed on mouse femurs, tibiae, pelvis, spleen, and peripheral blood. Harvested bones were crushed with a mortar and pestle and then filtered into single cell suspensions. Bone marrow, spleen and peripheral blood suspensions were red blood cell lysed and blocked with mouse Fc block (BD Biosciences, Cat#553142) and human IgG (Millipore Sigma, Cat#I4506) and then stained with fluorochrome-conjugated antibodies specific to human hematopoietic cells. For myelo-lympho engraftment analysis, cells from mice were stained with CD45 (HI30) (ThermoFisher, Cat#MHCD4528), CD33 (P67.6) (BD Biosciences, Cat#347787) and CD19 (HIB19) (BD Biosciences, Cat#555415). Analysis of human HSPC chimerism was performed using antibodies specific to CD38 (HB7) (BD Biosciences, Cat#335790) and CD34 (581) (BD Biosciences, Cat#555821) and CD133. Live cells were discriminated on the basis of cell size, granularity and, as needed, absence of viability dye 7-AAD uptake. All cord blood and mouse bone marrow flow cytometry analysis were performed using a BD LSR II instrument (BD Biosciences). Data acquisition was conducted using BD FACSDiva software (BD Biosciences) and analysis was performed using FlowJo software (Tree Star).

METHOD DETAILS

CellectSeq Selections

Phage-displayed fragment antibody (Fab) Library F was used to perform the Cellectseq selections (Persson et al., 2013). At the time that the selections were performed, the preparation of Library F had a diversity of 3×10^{10} and the stock used was diluted to 8×10^{12} cfu/mL (colony forming units). After precipitation and resuspension of Library F, it was calculated that each cell line was exposed to 100x the diversity of the library. This mixture was incubated on ice for 20 minutes, centrifuged for 20 minutes at 20,000 g and resuspended in binding buffer (DMEM (ThermoFisher, Cat#11995073) containing 10% FBS (Wisent, Cat#098-150), 50 mM HEPES (Millipore Sigma, Cat#15630080, 2 mM EDTA (Millipore Sigma, Cat#20158)). Libraries F was subjected to four rounds of selection with each round consisting of a pre-absorption step followed by a positive selection step. For the pre-absorption step, HEK293 cells were washed once with PBS and lifted with a gentle EDTA solution (0.3 g/L disodium EDTA (Millipore Sigma, Cat#20158), 8 g/L NaCl (Millipore Sigma, Cat#5886), 0.56 g/L sodium bicarbonate (Millipore Sigma, Cat#S5761), 1 g/L D-glucose (Millipore Sigma, Cat#G7021), 0.4 g/L KCl (Millipore Sigma, Cat#60142) and resuspended in DMEM with 10% heat inactivated FBS. Ten million cells were then resuspended with approximately 1012 cfu of either library F phage in a cell-binding buffer. The cells were incubated with the library for 1.5 hours at 4°C with gentle rocking. The cells were then centrifuged for 5 minutes at 1500 rpm and the supernatant containing unbound phage was used for the positive selection. In the positive selection, HEK293 cells stably overexpressing CD133 were harvested in the same manner as cells in the pre-absorption step and 5 million cells were resuspended with pre-adsorbed Library F. Cells were incubated with the library for 2 hours at 4°C with gentle rocking. Following incubation, cells were centrifuged for 5 minutes at 1500 rpm. The supernatant was removed, and the cells were washed with 10 mL cold PBS and transferred to a new tube after which the cells were again centrifuged for 5 minutes at 1500 rpm. This washing process was repeated three times. After the last wash cells were pelleted and wash buffer was completely removed. The cell pellets were incubated with 0.1N HCL (Millipore Sigma, Cat#H1758) for 5 minutes at room temperature to elute the phage particles. The eluate was neutralized with 1M Tris-HCl (Millipore Sigma, Cat#T5941). Half of the elution was used to infect actively growing XL1-blue *E. coli* cells (Agilent Cat# 200249) for 30 minutes at 37°C. After the initial infection, XL1-blue cells were co-infected with M13K07 at a final concentration of 1010 pfu and incubated for 45 minutes at 37°C. After the co-infection period, infected cells were transferred to a 25 mL flask of 2YT culture medium (ThermoFisher Cat#22712020) with 100 μg/mL carbenicillin (GIBCO Cat#10177012) and 25 μg/mL kanamycin (GIBCO, Cat#11815032) and grown overnight. The next day, the cells were pelleted, and the phage was precipitated from the supernatant using PEG/NaCl. This phage was used in a second round of re-absorption and positive selection after which the entire process was repeated for two more rounds of selection. In parallel, a negative selection was performed on parental HEK293 cells by eluting the phage from the pre-adsorption step, neutralizing this phage and infecting XL1-blue cells with a portion of this eluate. This process was started at selection round 2.

Cell-based ELISA

Single colonies of phage-fab or phage-scFv-infected XL1-blue cells were picked, inoculated into 350ul 2YT containing 100 μg/mL carbenicillin and 25 μg/mL kanamycin and allowed to grow overnight at 37°C. The same day, two 96-well tissue culture treated Costar plates were treated with 50 μg/mL poly-L-lysine (Sigma) for 10 minutes at Room temperature in the tissue culture hood. Coated wells were washed once with PBS and 50,000 HEK293 or HEK293-CD133 cells were seeded per well and allowed attach to the plate overnight. After 24 hours, the bacterial cultures were spun down and 50ul of culture supernatant was added to a HEK293/HEK293-CD133 pair of wells (each clone picked was added to a well with HEK293 cells as a control and a HEK293-CD133 well to test for binding). Cells were incubated with the phage for 1.5 hours at 37°C. After the incubation period, the media was removed and the cells were washed twice with PBS. The cells were subsequently fixed with 3.2% Paraformaldehyde (PFA, Electron Microscopy Sciences, Cat# RT15700) for 20 minutes at room temperature. The cells were then washed and blocked with a PB buffer (0.2%BSA in PBS) and incubated with anti-M13 conjugated to Horseradish peroxidase (anti-M13-HRP, Abcam Cat# ab50370) at a 1:5000 dilution for 30 minutes at room temperature. After the incubation period, the cells were washed three times with PBS with five-minute incubations between each wash. The plate was developed by adding 50 μL of a 1:1 mixture of TMB Peroxidase substrate and Peroxidase substrate solution B (KPL) (Seracare, Cat#5120-0047) and incubating at room temperature for 5-10 minutes. The reaction was stopped with 50 μL 1M Phosphoric acid (Millipore Sigma, Cat #695017).

Secondary sphere formation assay

Tumorspheres were dissociated using 5-10μL Liberase Blendzyme3 (0.2 Wünsch unit/mL) in 1mL PBS for 5 min at 37°C. Cells were plated at 200 cells per well in 200 μL of NCC media in a 96-well plate. The cells were treated with RW03 (20nM- 5μM) or IgG control AffiniPure Goat Anti-Human IgG, F(ab')2 fragment specific, Jackson ImmunoResearch, Cat#109-005-006). Cultures were left undisturbed at 37°C, 5% CO_2. After four days, the number of secondary spheres formed were counted.

Cell proliferation assay

Single cells were plated in a 96-well plate at a density of 1,000 cells/200 μL per well in quadruplicate treated with RW03 (20 nM- 5μM) or IgG control and incubated for five days. 20 μL of Presto Blue (ThermoFisher, Cat#A13262), a fluorescent cell metabolism indicator, was added to each well approximately 4h prior to the readout time point. Fluorescence was measured using a FLUOstar Omega Fluorescence 556 Microplate reader (BMG LABTECH) at excitation and emission wavelengths of 535 nm and 600 nm respectively. Readings were analyzed using Omega analysis software.

Generation of CAR Lentivirus

Human anti-CD133 (RW03) scFv sequence was synthesized with a 5′ leader sequence and 3′ Myc tag by Genescript. The scFv was cloned into the lentiviral vector pCCL ΔNGFR (kindly provided by Dr. Bramson, McMaster University, Hamilton, ON, Canada) downstream of the human EF1α promoter leaving ΔNGFR intact downstream of the minimal cytomegalovirus promoter. Empty pCCL ΔNGFR was used as a control vector. Replication-incompetent lentiviruses were produced by co-transfection of the CAR vectors and packaging vectors pMD2G and psPAX2 in HEK293FT cells using Lipofectamine 3000 (ThermoFisher, Cat#L3000075) as recommended by the manufacturer. Viral supernatants were harvested 48 hours after transfection, filtered through a 0.45 μm cellulose acetate filter (Millipore Sigma, Cat#SE1M002M00) and concentrated by ultracentrifugation at 15,000 RPM for 2h at 4°C. The viral pellet was resuspended in 1.0 mL of T cell media, aliquoted and stored at −80°C.

Generation of CAR-T cells

Peripheral blood mononuclear cells (PBMCs) from consenting healthy blood donors were obtained using SepMate™ (STEMCELL technologies, Cat#85450). This research was approved by the McMaster Health Sciences Research Ethics Board. 1 × 10⁵ cells in XSFM media (Irvine Scientific, Cat#91141) were activated with anti-CD3/CD28 beads at a 1:1 ratio (Dynabeads, GIBCO, Cat#113.31D) in a 96-well round bottom plate with 100U/mL rhIL-2 (Peprotech, Cat#200-02) and 10 ng/mL rhIL-7 (Peprotech, Cat200-07). Twenty-four hours after activation, T cells were transduced with lentivirus at an MOI~1. CAR-T cell cultures were expanded into fresh media (XSFM media supplemented with 100U/mL rhIL-2 and 10 ng/mL rhIL-7) as required for a period of 12–15 days prior to experimentation.

Activation assays and Evaluation of cytokine release

NGFR+ sorted CAR-T cells (CAR-CD133 or CAR-CON) were co-incubated with GBM cells at a 1:1 ratio for 24 hours. GBM cells and T cells were incubated at a 1:1 ratio with or without CD133 DATEs (1μg). The CAR-T cells and T cells were analyzed for activation markers CD25 (Miltenyi Biotech, Cat#130-113-283) and CD69 (Miltenyi Biotech, Cat#555533) by Flow cytometry. Supernatants were collected and stored at −80°C for analysis of cytokines. Cytometric Bead Array (CBA) Kit (BD Biosciences, Cat#550749) was used for flow cytometry quantification of the different cytokines, according to manufacturer's description. Briefly, in each tube 50μL of either Cytokine Standards dilution or supernatant, 50μL of Cytokine Capture Beads and 50uL of PE Detection Reagent was added. After 3h incubation at room temperature in the dark, the beads were washed and acquired on a MoFlo XDP flow cytometer (Beckman Coulter), properly setup using Cytometer Setup Beads.

T cell proliferation

NGFR+ CAR T (CART133 or CAR CON), or T cells with and without DATEs (1μg), were incubated with GBM cells. After 24 hours of incubation, cells were collected, CD3+ T cells were sorted into 96 well plates and analyzed for proliferation after 3 days using the Presto Blue assay.

Cytotoxicity assays

Luciferase-expressing GBM cells at a concentration of 30,000 cells/well were plated in 96–well plates in triplicates. In order to establish the BLI baseline reading and to ensure equal distribution of target cells, D-firefly luciferin potassium salt (100 mg/mL) was added to the wells, and measured with a luminometer (Omega). Subsequently, effector cells were added at 4:1, 2:1, 1:1, and 0:1 effector-to-target (E:T) ratios and incubated at 37°C for 4-8 hours. BLI was then measured for 10 s with a luminometer as relative luminescence units (RLU). Cells were treated with 1% Nonidet P-40 (NP40, Thermofisher, Cat#98379) to measure maximal lysis. Target cells incubated without effector cells were used to measure spontaneous death RLU. The readings from triplicates were averaged and percent lysis was calculated with the following equation:

$$\% \textit{ Specific lysis} = 100X(\textit{spontaneous death RLU} - \textit{test RLU})/(\textit{spontaneous death RLU} - \textit{maximal killing RLU}).$$

Flow cytometric analysis and sorting

GBM cells in single cell suspensions and T cells were resuspended in PBS+2mM EDTA. GBM cells were stained with APC-conjugated anti-CD133 or a matched isotype control (Miltenyi Biotech, Cat#130-112-158), RW03 followed by anti-human Alexa 488 conjugated secondary antibody (Jackson ImmunoResearch, Cat#109-546-097), CD133 DATEs (15min RT) followed by anti-human Alexa 488 conjugated secondary antibody and incubated for 30 min on ice. T cells were stained with CD133 DATEs (15min RT) followed by anti-human Alexa 488 conjugated secondary antibody. CAR-T cells were stained with fluorescent tagged anti-CD3 (BD Biosciences, Cat#557851), anti-CD25 (Miltenyi Biotech, Cat#130-113-283), anti-CD69 (BD Bioscienecs, Cat#555533), anti-NGFR (Miltenyi Biotech, Cat#130-112-790) and anti-c-Myc (Miltenyi Biotech, Cat#130-116-653). Samples were run on a MoFlo XDP Cell Sorter (Beckman Coulter). Dead cells were excluded using the viability dye 7AAD (1:10; Beckman Coulter, A07704). Compensation was performed using mouse IgG CompBeads (BD Biosciences, Cat#552843). NGFR+ CAR-T cells were sorted into tubes containing 1mL XSFM media and small aliquots of each sort tube were re-analyzed to determine the purity of the sorted populations. Cells were allowed to equilibrate at 37°C for a few hours prior to use in experiments.

RW03 Antibody quantification in brain tissue

RW03 modification Cy7-sulfo-NHS ester (4.6 μL of 10 mg mL^{-1} in DMSO) (Lumiprobe, Cat#15320) was added to 300 μL of RW03 (5.5 mg mL^{-1}) in PBS with 20% glycerol (Millipore Sigma, Cat#G5516) and reacted overnight at 4°C in the dark. The reaction was then transferred to a dialysis membrane (MWCO 12-14k) (Spectrapor, Cat#08-667A) and dialyzed against PBS with 10% glycerol for 3 d with 3 exchanges at 4°C in the dark. The fluorescent antibody solution was sterilized with a 0.2 μm spin filter (Millipore Sigma, Cat#CLS8160). RW03 (50 μg) was injected into brains of mice and they were extracted at specified time points (30 min, 2h, 6h, 24h and 48h; n = 3 per group) and flash frozen with liquid nitrogen until further use. Brains were thawed, weighed and transferred to 2 mL screw cap vials containing zirconium beads (BioSpec, Cat#11079110z, Cat#10832). The brains were then homogenized using a Mini-BeadBeater 16 (BioSpec, Cat#607) for 1.5 min. 500 μL PBS was then mixed to the homogenized brains and 100 μL of the mixture was pipetted onto a black 96 well plate. RW03-Cy7 was detected using a Tecan Infinite M200 Pro (ex. 750 nm, em. 780 nm). Concentrations of RW03-Cy7 in each sample was determined with a calibration curve with known amounts of RW03-Cy7.

QUANTIFICATION AND STATISTICAL ANALYSIS

Statistical Analysis

Biological replicates from at least three patient samples were compiled for each experiment, unless otherwise specified in figure legends. Respective data represent mean ± SD, *n* values are listed in figure legends. Student's t test analyses, 2-way ANOVA with Bonferroni post hoc tests, and Log-rank (Mantel-Cox Test) analysis were performed using GraphPad Prism 5. $p > 0.05$ = n.s., $p < 0.05$ = *, $p < 0.01$ = **, $p < 0.001$ = ***, $p < 0.0001$ = ****.

ADDITIONAL RESOURCES

None